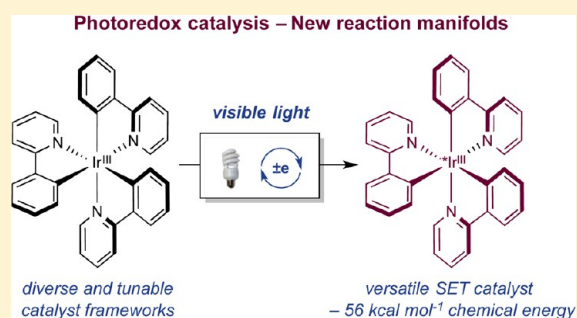# Photoredox Catalysis in Organic Chemistry

Megan H. Shaw, Jack Twilton, and David W. C. MacMillan*

Merck Center for Catalysis at Princeton University, Princeton, New Jersey 08544, United States

ABSTRACT: In recent years, photoredox catalysis has come to the forefront in organic chemistry as a powerful strategy for the activation of small molecules. In a general sense, these approaches rely on the ability of metal complexes and organic dyes to convert visible light into chemical energy by engaging in single-electron transfer with organic substrates, thereby generating reactive intermediates. In this Perspective, we highlight the unique ability of photoredox catalysis to expedite the development of completely new reaction mechanisms, with particular emphasis placed on multicatalytic strategies that enable the construction of challenging carbon−carbon and carbon−heteroatom bonds.

Photoredox catalysis – New reaction manifolds

diverse and tunable catalyst frameworks — visible light ±e — versatile SET catalyst – 56 kcal mol⁻¹ chemical energy

INTRODUCTION

Over the last century, the discovery, development, and use of light-mediated catalysis has enabled the invention of a wide variety of nontraditional bond constructions in organic chemistry. More recently, the field of photocatalysis has undergone a significant renaissance, and once again, a series of new activation modes have in turn seeded a large variety of new bond-forming protocols and synthetic methodologies.[1] Photocatalysis, the field, encompasses an ever-increasing number of generic activation modes in which photonic energy is selectively targeted to a specifically designed photon-absorbing catalyst (a photocatalyst) which, upon excitation, is able to induce an accompanying substrate, reagent, or secondary catalyst to participate in unique reaction pathways that were previously unattainable under thermal control. The most common mechanisms by which photocatalysts are able to convert light into chemical energy and at the same time perform selective molecule activation include (i) energy transfer, (ii) organometallic excitation, (iii) light-induced atom transfer, and (iv) photoredox catalysis, all of which will be discussed in detail in this special issue. For the purposes of this Perspective, however, we will focus our discussion only on the impact and utility of photoredox catalysis as applied to organic synthesis. First, we will examine the utility of photoredox catalysis from a historical viewpoint, and thereafter, we will discuss the remarkable recent impact of this area on the field of organic reaction invention and its application in both industrial and academic settings. As the coverage of this paper cannot be (and is not intended to be) comprehensive, particular emphasis has been placed on reports that demonstrate the unique characteristics of photoredox catalysis and at the same time the truly novel nature of the accompanying reactions it can deliver.

Over the last four decades, photoredox catalysis has found widespread application in the fields of water splitting,[2] carbon dioxide reduction,[3] and the development of novel solar cell materials;[4] however, only recently has the potential of applying this catalytic platform to organic synthesis begun to be fully realized. A key factor in the recent yet rapid growth of this activation platform has been the recognition that readily accessible metal polypyridyl complexes and organic dyes can facilitate the conversion of visible light into chemical energy under exceptionally mild conditions. Upon excitation, these molecules can engage in single-electron transfer (SET) events with organic (and organometallic) substrates, providing facile access to open-shell reactive species.[5] Here, irradiation with visible light, at wavelengths where common organic molecules do not absorb, effects selective excitation of the photoredox catalyst. The resultant excited species can act as both a strong oxidant and a strong reductant simultaneously, thereby providing access to a reaction environment that is unique for organic chemistry (Figure 1). Indeed, this electronic duality contrasts directly with traditional redox reaction manifolds (e.g., electrochemistry) wherein the reaction medium can be either oxidative or reductive (but not both) and, in turn, provides access to previously inaccessible redox-neutral reaction platforms.

Recent advances in modern photoredox catalysis have enabled the development of a wide array of novel synthetic methodologies. Unprecedented forms of new reactivity are often observed with photoredox catalysis in comparison with traditional reaction manifolds, a feature that can be attributed to both the aforementioned ability of photoredox catalysts to act as both an oxidant and reductant simultaneously in their excited states and their capacity to convert visible light into significant levels of chemical energy (e.g., the triplet state of Ir(ppy)$_3$ is 56 kcal mol⁻¹ above the ground state).[6] The combination of these capabilities has wide-reaching implications for the design of new synthetic transformations and provides the opportunity to access previously elusive or unknown mechanistic pathways.

- Max absorption at 375 nm (visible light)

- Long-lived excited state (τ = 1.9 μs)

- Single-electron transfer catalyst

- Effective oxidant and reductant

- Triplet energy of 56 kcal mol^{-1}

Ir(ppy)$_3$

reductant
$E_{1/2}^{IV/*III}$ = −1.73 V

Ir(ppy)$_3^+$

375 nm
MLCT
ISC

oxidant
$E_{1/2}^{*III/II}$ = +0.31 V

Ir(ppy)$_3^-$

Ir(ppy)$_3$
ground state

***Ir(ppy)$_3$**
excited state
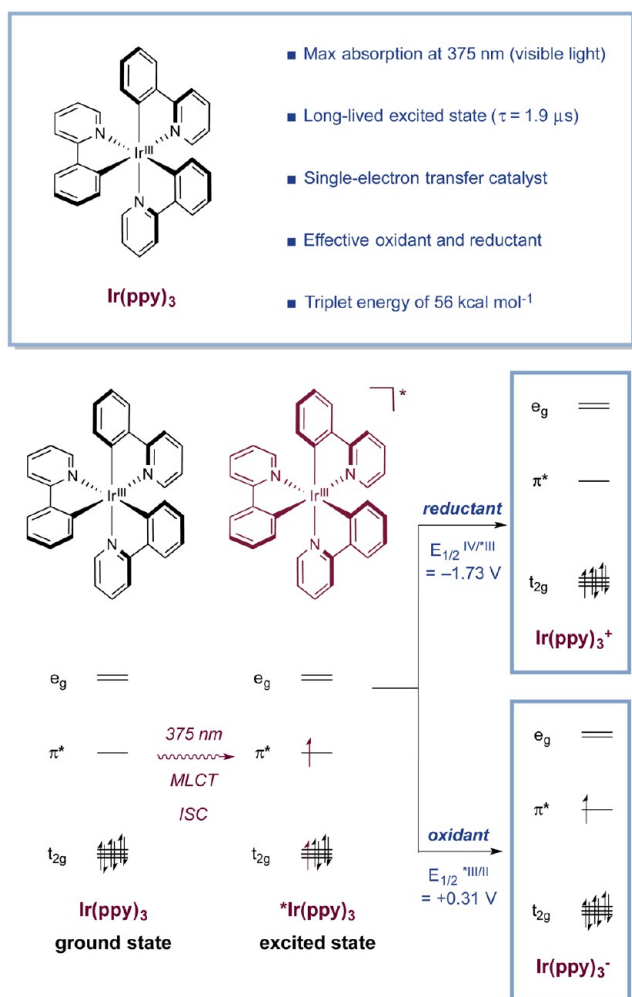
Figure 1. Iridium polypyridyl complexes: simplified molecular orbital depiction of Ir(ppy)$_3$ photochemistry.

Moreover, the development of multicatalytic strategies incorporating photoredox catalysis with a secondary catalyst system has gained significant attention as multisubstrate activation can be achieved when two discrete catalytic platforms are successfully interfaced. In this Perspective, we aim to highlight reports that demonstrate the unique aspects of photoredox catalysis and, in particular, emphasize novel bond disconnections and technologies which we anticipate will be broadly applicable in academic and industrial settings.

EARLY WORK

The first applications of photoredox catalysis to organic synthesis were reported almost 40 years ago, and these seminal publications laid the foundations for the recent developments in the field of modern photoredox catalysis. In 1978, Kellogg demonstrated that the photomediated reduction of sulfonium ions to the corresponding alkanes and thioethers, using *N*-substituted 1,4-dihydropyridines as the terminal reductant, could be accelerated by addition of a catalytic amount of [Ru(bpy)$_3$]Cl$_2$ (Scheme 1a).[7] Subsequent reports by Fukuzumi and Tanaka[8] and Pac[9] established that similar [Ru(bpy)$_3$]Cl$_2$−dihydropyridine catalyst systems could facilitate the reduction of a wide range of organic substrates, including electron-deficient olefins, aromatic ketones, and benzylic and phenacyl halides.

In 1984, Cano-Yelo and Deronzier reported the first net oxidative photoredox-catalyzed reaction using aryldiazonium salts as the terminal oxidant for the conversion of benzylic alcohols to the corresponding aldehydes.[10] Shortly after, they disclosed the first redox-neutral photoredox-catalyzed trans-formation.[11] Here, it was found that the Pschorr reaction could be catalyzed by [Ru(bpy)$_3$]Cl$_2$, resulting in a quantitative yield of the phenanthrene product (Scheme 1b). Notably, it was observed that the reaction proceeded with much higher quantum efficiency under photoredox catalysis conditions compared with direct photolysis of the reaction mixture.

Pioneering studies by Okada and co-workers demonstrated that *N*-(acyloxy)phthalimides, which can be readily prepared from the corresponding carboxylic acid, could be used as a convenient source of alkyl radicals. Following single-electron reduction, the redox-active ester fragments to deliver phthalimide (after protonation), carbon dioxide, and the corresponding carbon-centered radical. In the initial report from Okada regarding visible light-mediated fragmentation, the generated C-centered radicals engaged in conjugate additions with Michael acceptors.[12] Okada demonstrated that alkyl radicals formed via reductive fragmentation of redox-active esters could be utilized in a variety of transformations, including chlorination, phenylselenenylation, and hydrogen atom ab-straction from *tert*-butyl thiol to furnish the fully reduced alkane
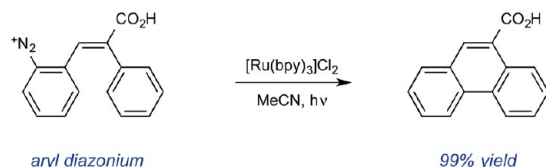
Scheme 1. Seminal Contributions to Organic Photoredox Catalysis
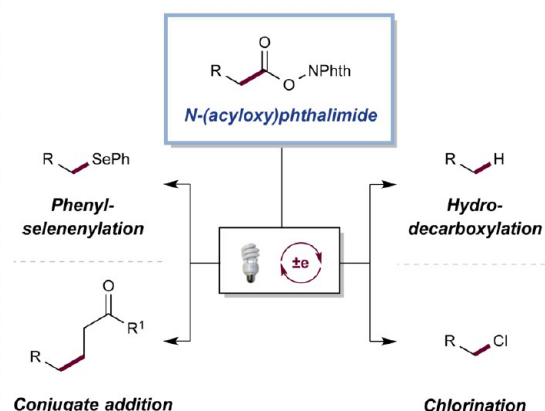

(a) *Kellogg, 1978 – Reductive desulfuration*
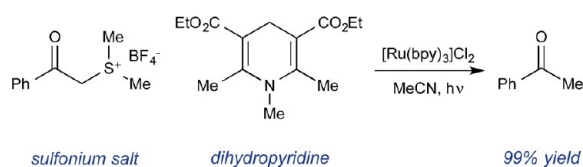
sulfonium salt   dihydropyridine   99% yield   Richard Kellogg

(b) *Deronzier, 1984 – Photocatalytic Pschorr reaction*

aryl diazonium   99% yield   Alain Deronzier

(c) *Okada – Reductive decarboxylation of redox-active esters*

N-(acyloxy)phthalimide

Phenyl-selenenylation

Hydro-decarboxylation

Conjugate addition

Chlorination

(Scheme 1c).[13] The strategy outlined in this series of reports represents the first general photoredox-mediated mode of substrate activation. Despite this early demonstration of the potential of photoredox catalysis for application to organic synthesis, the area remained relatively underappreciated by the broader community until the late 2000s.

In 2008, Yoon and co-workers disclosed a photoredox-catalyzed intramolecular [2 + 2] enone cycloaddition reaction (Scheme 2a).[14] In this seminal study, a Lewis acid additive was employed to modulate the reactivity of the enone substrate, demonstrating the beneficial effect of combining two activation modes in one sequence. At the same time, our laboratory developed a dual photoredox organocatalytic protocol for the enantioselective α-alkylation of aldehydes (Scheme 2b).[15] This reaction exploited the unique properties of photoredox catalysis to generate electron-deficient radicals that can combine with catalytically generated enamines in a highly enantioselective fashion, thereby providing one solution to the long-standing asymmetric α-carbonyl alkylation challenge. Shortly afterward, Stephenson and co-workers reported a mild reductive dehalogenation protocol for benzylic and α-acyl halides (Scheme 2c).[16] Importantly, under photoredox-catalyzed conditions, this transformation could be conducted without the use of toxic tin reagents. These three reports collectively underscored the potential of this mode of activation as a valuable catalysis platform for organic reaction development and helped reinitiate a significant growth in the field of photoredox catalysis. Since these early reports, a wide range of Rh and Ir polypyridyl complexes, as well as various organic dyes, have been demonstrated as efficient catalysts for the conversion of visible light to chemical energy (Figure 2). In this regard, the ability to tune the properties of such metal complexes through modification of the ligand backbone has significantly expanded the repetoire of synthetic transforma-

tions that can be accomplished using photoredox catalysis, thereby enhancing further interest in the field. Indeed, as demonstrated in Figure 3, there has been an exponential increase in the number of publications that employ photoredox catalysis since the late 2000s,[17] giving rise to a diverse and highly active field of research that continues at the present time.

■ AMINE α-FUNCTIONALIZATION

Nitrogen heterocycles represent a privileged motif in natural products and biologically active compounds,[18] as such synthetic chemists have long focused their efforts on the functionalization and construction of these important ring systems. In this regard, developments in the field of photoredox catalysis have delivered a wide array of synthetic strategies for site selective α-functionalization of amines. Founded upon early work from the Stephenson group, who disclosed a photoredox-catalyzed aza-Henry reaction in 2010 (Scheme 3),[19] a general oxidative activation mode has arisen for N-arylamines. In these transformations, reductive quenching of the excited state of the photocatalyst by an amine (**1**) generates an amine radical cation (**2**). Following this step, the α-amino C−H bonds become relatively acidic and can be readily removed by a weak base to generate an α-amino radical.[20] Subsequently, this radical can be oxidized to an iminium ion (**3**), a step in which a wide variety of terminal oxidants have been shown to be competent. An alternate mechanistic pathway is presented in Scheme 3, wherein amine radical cation **2** undergoes α-amino C−H abstraction by a radical anion (arising via reduction of an oxidant by the photocatalyst) to generate the same iminium species (**3**). In the initial report by Stephenson, the resultant electrophilic iminium ions were trapped with nitroalkanes to deliver the corresponding α-functionalized products. This strategy has proven general for a wide range of nucleophilic coupling partners including malonates,[21] cyanide,[22] trifluoromethyl anion,[22] electron-rich aromatics,[23] and phosphonates[24] in addition to tethered amines and alcohols which forge the corresponding heterocycles via intramolecular cyclization[25] (Scheme 3).

The synergistic merger of this N-arylamine activation mode with other catalytic platforms has also been accomplished. In these protocols, in situ generation of the nucleophilic coupling partner is generally mediated by the second catalytic system (Scheme 4). For example, Rueping and co-workers reported a photoredox proline-catalyzed Mannich reaction, wherein catalytic generation of the iminium ion and an enamine precedes formation of the desired carbon−carbon bond.[26] Along similar lines, Rovis reported an organocatalytic asymmetric iminium acylation protocol wherein in situ generation of a Breslow-type intermediate was accomplished using a chiral N-heterocyclic carbene catalyst (**4**).[27] Subsequent trapping of the electrophilic iminium ion with this catalytic intermediate resulted in formation of the α-amino ketone products with high levels of enantioselectivity. Stephenson and Jacobsen demonstrated that the outlined N-arylamine activation mode could also be used in conjunction with anion-binding catalysis. By employing a ruthenium photoredox catalyst and chiral thiourea **5**, the authors were able to effect a two-step asymmetric Mukaiyama Mannich reaction.[28] In this reaction, the identity of both the oxidant and the photocatalyst counterion were key to achieving a highly enantioselective transformation. This effect was attributed to binding of the thiourea catalyst to the tightly associated halide counterion of the prochiral iminium ion, which consequently provides the

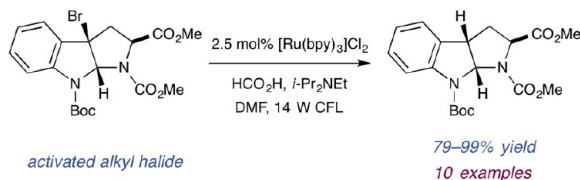## Scheme 2. Advent of Modern Organic Photoredox Catalysis

(a) Yoon, 2008 – [2+2] Enone cycloadditions
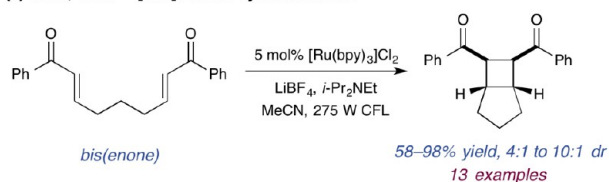
(b) 2008 – Asymmetric catalytic α–alkylation of aldehydes
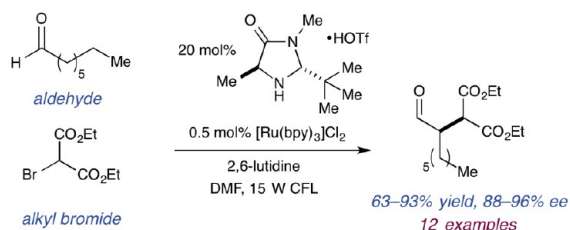
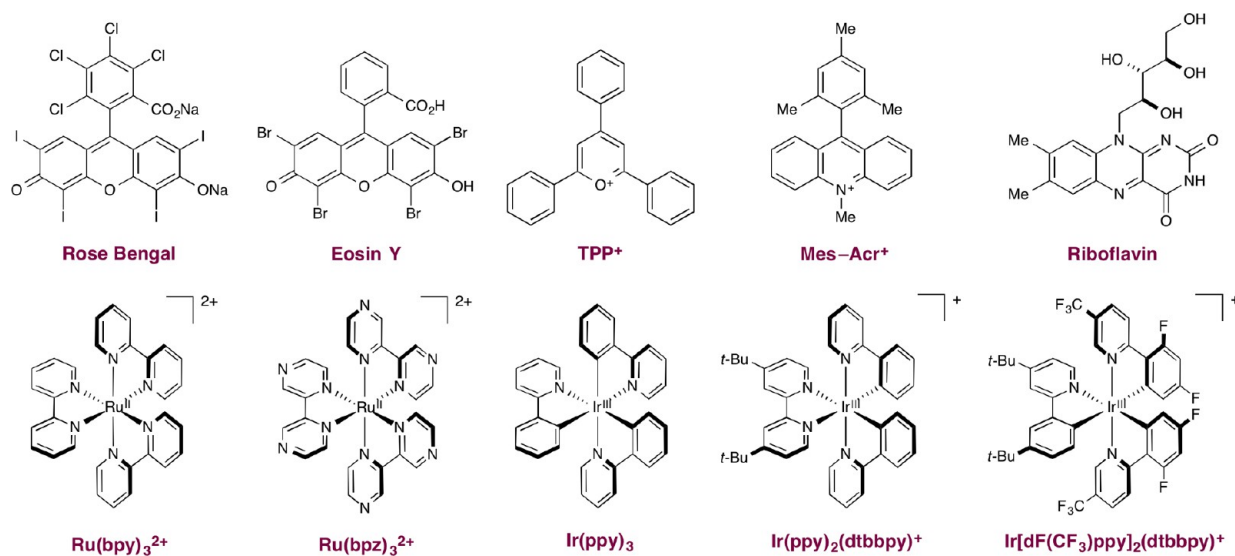(c) Stephenson, 2009 – Reductive dehalogenation of activated alkyl halides

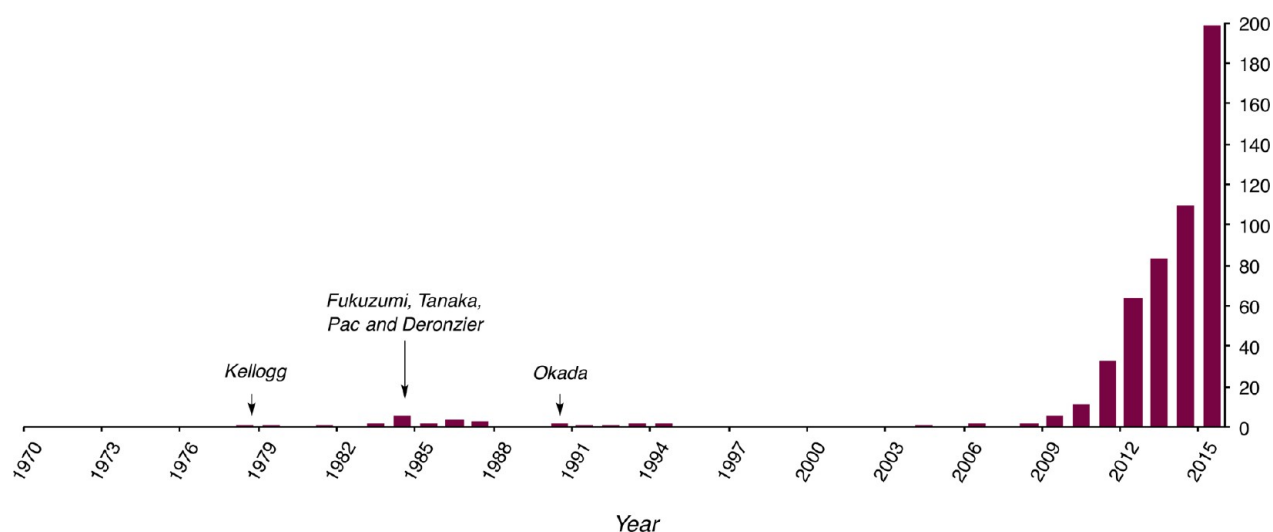**Figure 2.** Chemical structures of some common photoredox catalysts.

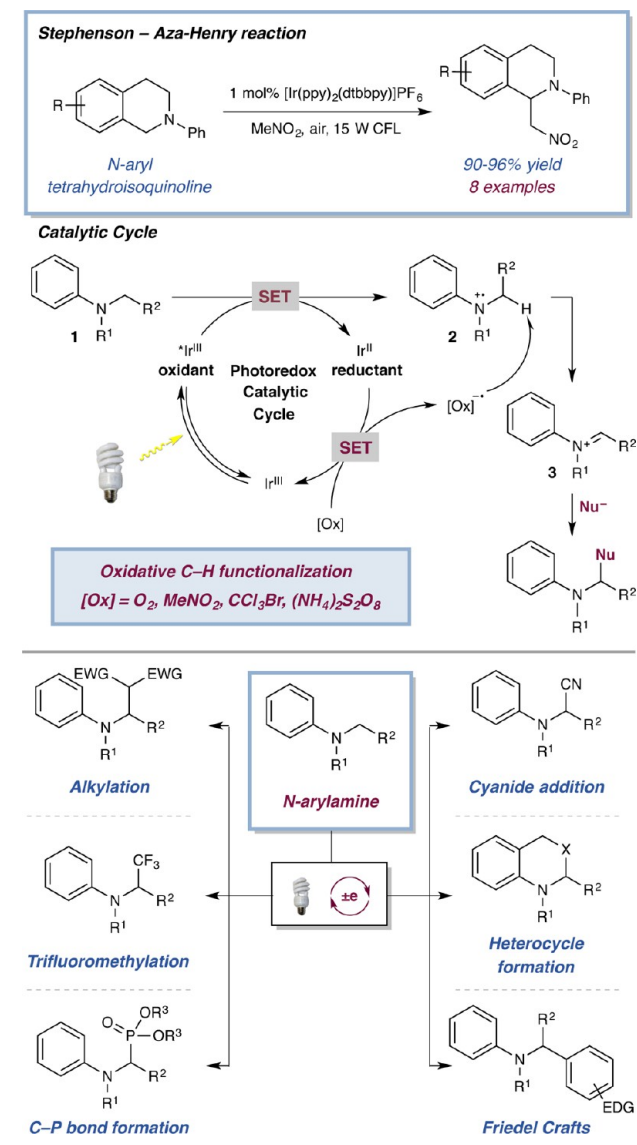**Figure 3.** Papers published per year in the field of organic photoredox catalysis.

desired enantiofacial discrimination in the nucleophilic addition step. In addition to the outlined protocols merging organo-catalysis with this activation mode, Rueping has shown that catalytically generated copper acetylides can also undergo addition to electrophilic iminium ions, demonstrating the feasibility of merging this activation mode with transition metal catalysis (vide infra).[29]

■ REDOX-NEUTRAL AMINE α-FUNCTIONALIZATION

In a complementary approach to the outlined oxidative amine functionalization platform, several groups have targeted the development of redox-neutral transformations wherein the initially generated nucleophilic α-amino radical (**6**) is trapped directly. In 2011, our laboratory reported a protocol for the direct arylation of α-amino C−H bonds using cyanoarenes as the coupling partner (Scheme 5).[30] In the proposed mechanism, initial reduction of the cyanoarene coupling partner by the highly reducing excited state of Ir(ppy)₃ generates radical anion **7** and the Ir(IV) state of the photocatalyst. The Ir(IV) species can readily oxidize N-arylamines, and the resulting radical cation (**8**) can then be
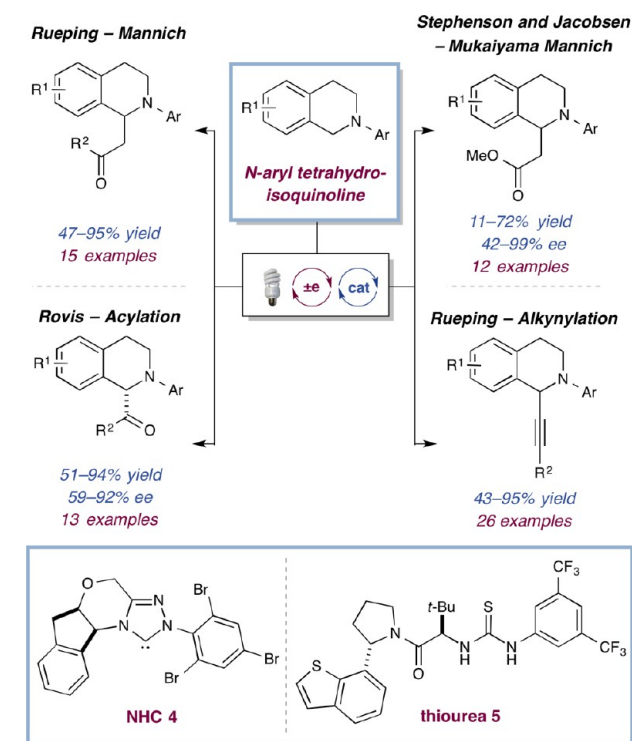
deprotonated by a weak base to generate the α-amino radical (**6**). Radical−radical coupling between the long-lived persistent cyanoarene radical anion **7** and the transient α-amino radical **6**, followed by elimination of cyanide, generates the benzylic amine products in a highly efficient manner. This general protocol is applicable to a wide range of arenes and heteroarenes, including pharmaceutically relevant five-membered heteroarenes, a class of compounds that are typically difficult to introduce via conventional coupling technologies.

Subsequently, the Nishibayashi group reported a mechanistically similar reaction for the synthesis of aminals (Scheme 6a).[31] Here, radical−radical coupling reactions occur between α-amino radicals and the radical anion derived from single-electron reduction of di-tert-butyl azodicarboxylate. Following on from early work by Reiser and Pandey (Scheme 6b), the Rueping, Yoon, and Nishibayashi groups independently reported protocols for redox-neutral α-alkylations of N-arylamines.[32] In these protocols, the nucleophilic α-amino radical is intercepted by a Michael acceptor, which upon reduction of the resultant α-acyl radical results in formation of the alkylated product. Elegant work from the Yoon and

Scheme 3. Oxidative α-Amino Functionalization

Scheme 4. Union of Oxidative α-Amino Functionalization and Other Modes of Catalysis
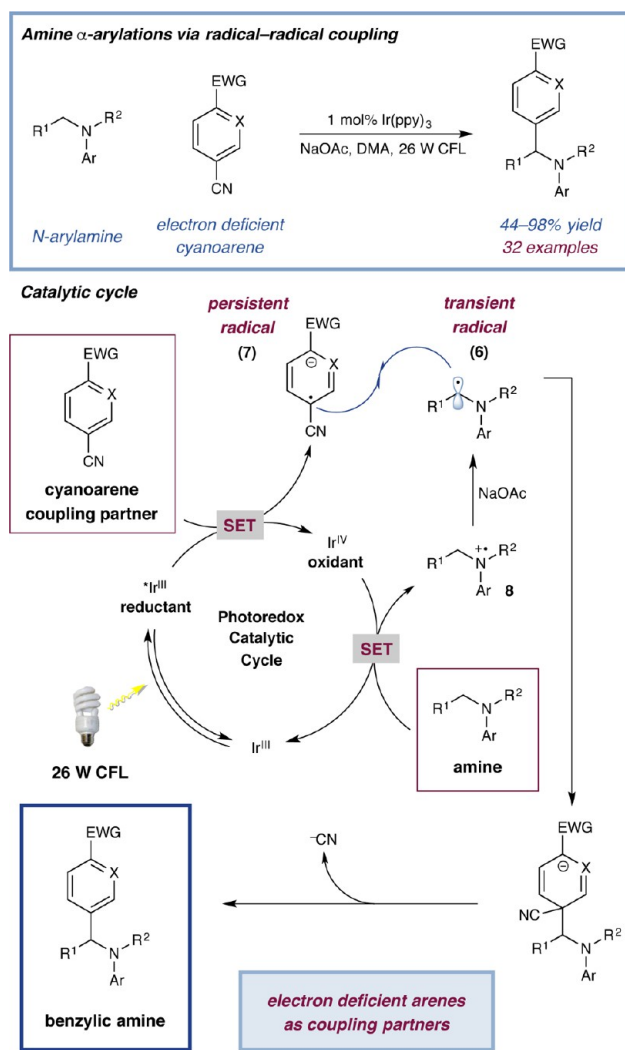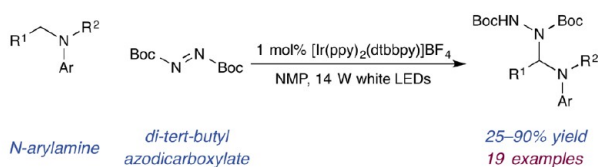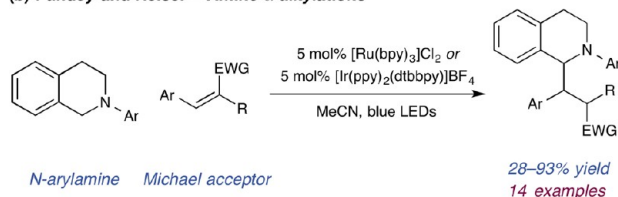

Several extensive reviews on photoredox-mediated amine functionalization have been published.[41]

DUAL PHOTOREDOX CATALYSIS PLATFORMS

In recent years, many research groups have focused on developing dual catalytic methodologies, which combine photoredox with a second catalytic activation mode. One of the unique aspects of photoredox catalysis is the ability to have both an oxidant and a reductant present in the reaction medium at the same moment. In dual catalytic systems, this characteristic can be particularly significant as turnover of the interdependent catalytic cycles can often rely on modulation of the oxidation states of transiently generated catalytic intermediates. Indeed, this intercycle reliance can prevent the generation of excess quantities of highly reactive species, an attractive mechanistic feature that is often overlooked in these redox-neutral processes. In the following sections, we highlight several catalytic activation modes that have been successfully interfaced with a number of photoredox mechanisms: namely organocatalysis, transition metal catalysis, and Lewis acid catalysis.

DUAL PHOTOREDOX ORGANOCATALYSIS: COVALENT ACTIVATION MODES

In our laboratory's initial report involving light-mediated activation, we outlined a novel dual photoredox organocatalysis strategy which enabled the enantioselective α-alkylation of aldehydes with α-bromo carbonyls (Scheme 8).[15] Here, the combination of enamine and photoredox catalysis enables simultaneous generation of a chiral enamine intermediate and a highly reactive electrophilic radical species in an overall redox-neutral manner. In this transformation, we proposed that in situ condensation of chiral secondary amine organocatalyst **9** with an aldehyde delivers nucleophilic enamine **10**. Subsequently,

Melchiorre groups has subsequently demonstrated that by using a chiral Lewis acid or organocatalyst respectively, these transformations can be rendered asymmetric (vide infra).[33,34]

Recent reports from our laboratory, Sammis, and others have demonstrated that C-centered radicals can also be accessed from carboxylic acid precursors through the use of photoredox catalysis. Here, oxidation of the corresponding carboxylate results in extrusion of CO_2 to deliver the desired alkyl radical species. The compatibility of this activation mode with amino acid derivatives enables facile access to α-amino radicals. This mode of radical generation is highly attractive as the carboxylic acid precursors are readily available, bench-stable compounds. In addition, a wide range of α-amino, α-oxy, benzylic, and simple alkyl radicals can be accessed using this strategy, with the carboxylic acid acting as a traceless activation handle. As a result, carboxylic acids have been exploited in a variety of redox-neutral transformations including decarboxylative fluorinations,[35] vinylations,[36] alkynylations,[37] and conjugate additions[38] as well as enabling hydrodecarboxylation[39] and radical–radical coupling reactions (Scheme 7).[40] Synthetic chemists have rapidly adopted the strategies discussed in this section as functionalized amine products are valuable pharmacophores.

Scheme 5. Photoredox-Catalyzed α-Amino C−H Arylations via Radical−Radical Coupling

Amine α-arylations via radical–radical coupling

N-arylamine   *electron deficient cyanoarene*   *44–98% yield* *32 examples*

Catalytic cycle

persistent radical (7)   transient radical (6)

cyanoarene coupling partner

SET   Ir^IV oxidant

*Ir^III reductant

Photoredox Catalytic Cycle

SET

26 W CFL   Ir^III   amine

NaOAc

benzylic amine

electron deficient arenes as coupling partners

Scheme 6. Photoredox-Catalyzed Redox-Neutral α-Amino Functionalizations

(a) Nishibayashi – Amine α-aminations

N-arylamine   *di-tert-butyl azodicarboxylate*   *25–90% yield* *19 examples*

1 mol% [Ir(ppy)₂(dtbbpy)]BF₄
NMP, 14 W white LEDs

(b) Pandey and Reiser – Amine α-alkylations

5 mol% [Ru(bpy)₃]Cl₂ or
5 mol% [Ir(ppy)₂(dtbbpy)]BF₄
MeCN, blue LEDs

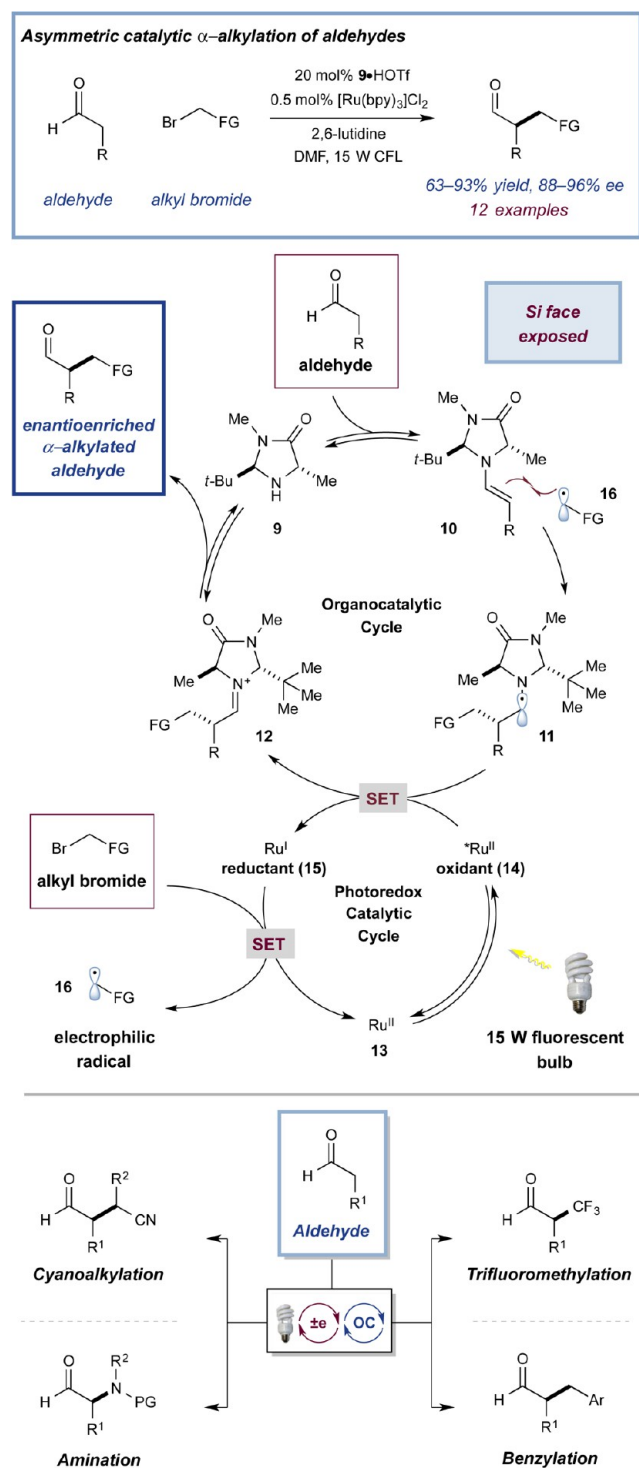*N-arylamine*   *Michael acceptor*   *28–93% yield* *14 examples*

enamine **10** can react in a highly enantioselective fashion with electrophilic radical **16**, generated via single-electron reduction of an activated alkyl halide by a Ru(I) photocatalyst (**15**), to deliver α-amino radical **11**. Intermediate **11** can be oxidized by the excited state of the Ru(II) photocatalyst (**14**), and finally,

Scheme 7. Decarboxylative Transformations Using Photoredox Catalysis

Fluorination   *carboxylic acid*   *Vinylation*

Conjugate addition   ±e   *Hydro-decarboxylation*

Radical-radical coupling   *Alkynylation*
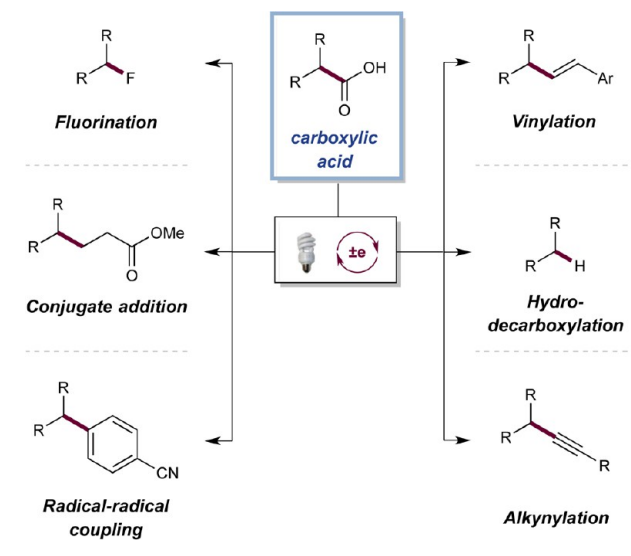
hydrolysis of the resultant iminium ion (**12**) closes the organocatalytic cycle. Since this initial publication, our laboratory has been able to expand this mechanistic platform to a wide range of asymmetric α-functionalization reactions including trifluoromethylation,[42] benzylation,[43] and cyanoalkylation (Scheme 8).[44] Additionally, a photomediated protocol for the α-amination of aldehydes was developed via the use of a photolabile group on the amine radical precursor.[45] Notably, in all these cases the mild reaction conditions allow stereocenters that are often susceptible to racemization to be generated in an enantioselective fashion. Following on from these reports, several other research groups have demonstrated the successful merger of enamine and photoredox catalysis. Luo and co-workers have developed a protocol for highly enantioselective α-alkylations of 1,3-dicarbonyls using a primary amine organocatalyst, thereby providing entry to enantioenriched quaternary stereocenters.[46] Moreover, several other groups have demonstrated that iron polypyridyl complexes and certain organic dyes can be used in place of ruthenium- and iridium-based photocatalysts in these reactions.[47]
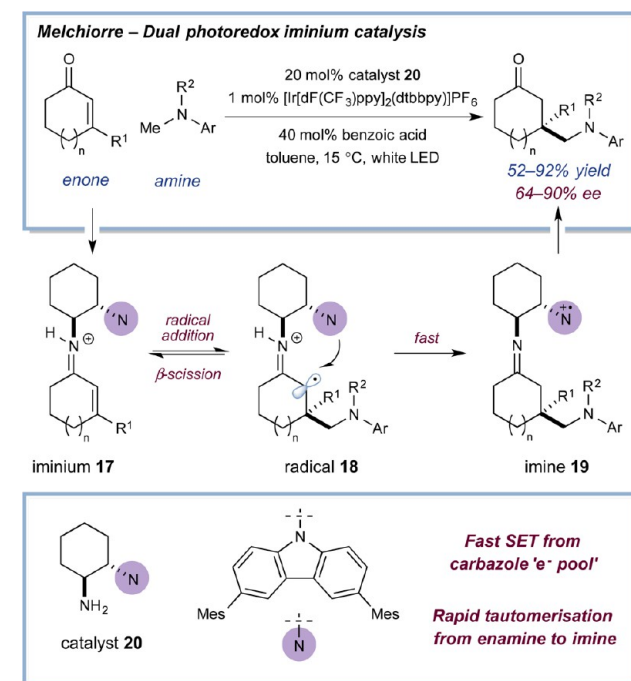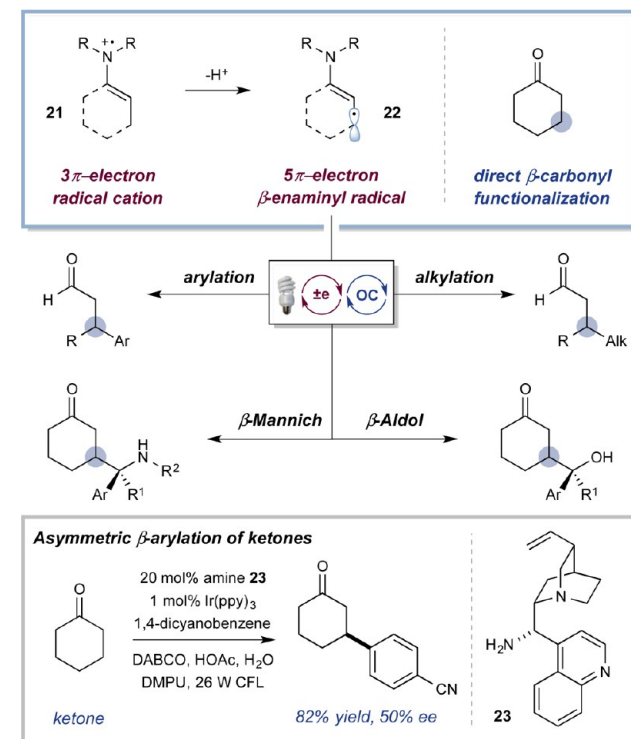
The merger of photoredox catalysis with other organocatalytic activation modes has expanded the repertoire of carbon−carbon and carbon−heteroatom bond-forming reactions that can be accomplished using this dual catalytic strategy. Recently, Melchiorre and co-workers were able to elegantly leverage the long-established LUMO lowering strategy of iminium catalysis to develop asymmetric conjugate additions of α-amino radicals, derived from N-arylamines, to α,β-unsaturated ketones (Scheme 9).[34] A key challenge in the development of radical conjugate additions to iminium ions is the propensity for the radical cation intermediates (such as **18**) to undergo β-scission to regenerate the iminium species (i.e., **17**).[48] To overcome this issue, chiral primary amine catalyst **20** was employed wherein rapid intramolecular electron transfer between the electron-rich carbazole and the α-iminyl radical cation functionality of **18** occurs, thereby delivering the corresponding enamine and precluding an undesirable β-scission event. Tautomerization to imine **19** thereafter impedes back-electron transfer, and consequently, this electron-relay strategy allows intermediate **18** to be rapidly converted to a homolytically stable product (**19**). The outlined photoredox

Scheme 8. Enantioselective α-Functionalization of Aldehydes via Dual Photoredox Organocatalysis

Scheme 9. Enantioselective Radical Conjugate Additions to Enones

Scheme 10. Direct β-Carbonyl Functionalization through the Merger of Photoredox and Organocatalysis

iminium dual catalysis platform enables challenging quaternary carbon stereocenters to be constructed in a highly enantioselective manner.

In 2007, a novel organocatalytic activation mode was introduced by our laboratory that enables enantioselective α-carbonyl functionalizations to be accomplished via trapping of a transiently generated electrophilic 3π-electron SOMO intermediate (**21**, Scheme 10).[49] In these initial reports, the SOMO species was formed via single-electron oxidation of an enamine

using stoichiometric oxidants. Koike and Akita demonstrated that photoredox catalysis can mediate the generation of the requisite SOMO species in the context of a catalytic α-oxygenation of aldehydes.[50] Here, the radical cation species undergoes radical–radical coupling with persistent radical TEMPO to furnish the α-oxygenated product.

Expanding on the established 3π-electron SOMO activation platform, we recently demonstrated that 5π-electron β-enaminyl radical intermediates **22** can be accessed via β-deprotonation of SOMO radical cation species **21**. Through the merger of organocatalysis and photoredox catalysis, this novel oxidative activation mode was combined with the previously reported strategy for reductive generation of persistent aryl radical anions (i.e., **7**, see Scheme 5) to enable selective redox-neutral radical–radical coupling reactions to be accomplished.[51] While catalytic intermediates such as enamines (i.e., **10**, see Scheme 8) and radical cations (**21**) provide access to α-functionalized carbonyl products, a well-established reaction manifold, enaminyl radicals **22** offer direct access to β-functionalized carbonyl adducts. Prior to this report, strategies for direct β-functionalization of saturated carbonyl compounds were rare, and as demonstrated by our subsequent reports (vide infra), this activation mode provides a general strategy for developing elusive β-functionalization protocols. Furthermore, when chiral amine catalyst **23** was employed, enantioenriched β-arylated cyclohexanones were formed, thereby establishing the feasibility of developing asymmetric radical–radical coupling reactions. This result challenged the long-standing belief that catalytic asymmetric radical–radical couplings are unattainable due to the disordered nature of and long partial bonds present in the transition state.[52]

The outlined β-enaminyl radical activation strategy has been extended to couplings with catalytically generated ketyl (from ketones) and α-amino (from imines) radicals to accomplish formal β-aldol and β-Mannich reactions, respectively (Scheme 10).[53,54] In addition, we have demonstrated that nucleophilic radical **22** can be trapped by closed-shell electrophiles, such as Michael acceptors, to generate β-alkylated aldehydes in good yield.[55] During the development of these transformations, the use of DABCO as base was identified as key for achieving high efficiencies. Mechanistic studies indicated that DABCO could also be functioning as an electron transfer agent and facilitating oxidation of the in situ generated enamine. Alternatively, the oxidized DABCO radical cation could undergo a hydrogen-atom transfer event with the enamine to generate radical **22** directly. Control experiments highlighted the importance of DABCO; excluding this reagent from three-component β-Mannich reactions resulted in the formation of traditional Mannich products. However, in the presence of DABCO, exclusive formation of β-functionalized products was observed.

■ DUAL PHOTOREDOX ORGANOCATALYSIS: NONCOVALENT INTERACTIONS

As highlighted in the previous section, photoredox-mediated methodologies that exploit covalent organocatalytic activation modes can access unique reactivity and, importantly, the covalently bound catalysts can confer high levels of stereocontrol in these transformations. Catalysts that coordinate with the substrate through noncovalent interactions can also exhibit precise control over the efficiency and/or enantioselectivity of the corresponding reaction and a number of key dual catalytic examples are discussed below. It should be noted that elegant work from Yoon, Stephenson, and Jacobsen, in the areas of Lewis acid and thiourea catalysis, respectively, are discussed elsewhere in this Perspective.

Seminal studies from Ooi and co-workers described a unique mechanistic pathway for the highly enantioselective synthesis of diamines from *N*-sulfonylaldimines and *N*-arylaminomethanes (Scheme 11).[56] The key radical–radical coupling step was

Scheme 11. Enantioselective Radical–Radical Couplings Utilizing a Chiral Brønsted Acid Co-catalyst

Ooi - Enantioselective Brønsted acid photoredox catalysis

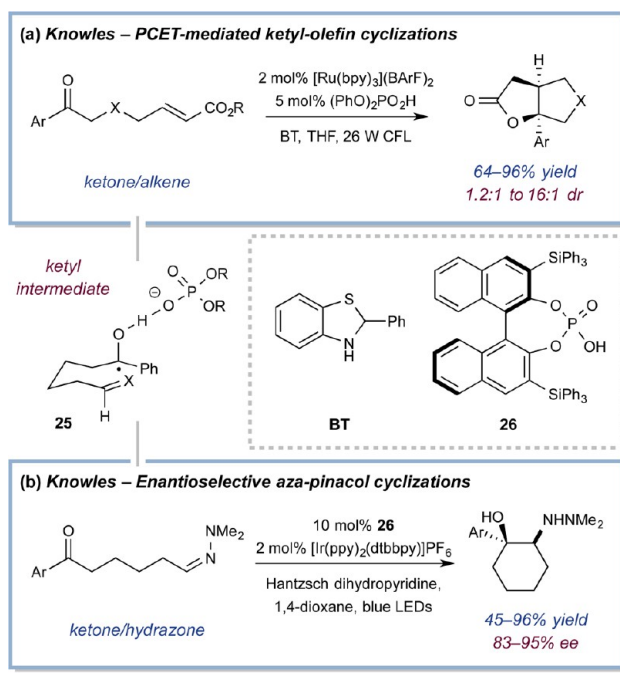**24**, Ar = 2-Ph-4-CF₃C₆H₃   *chiral ion pair*
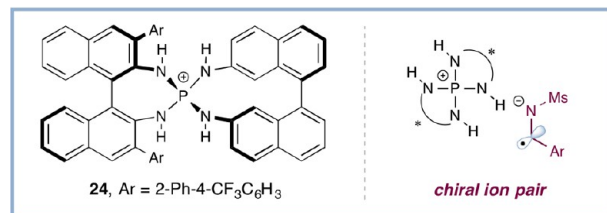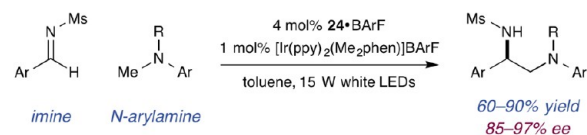
rendered asymmetric via the formation of a chiral ion pair consisting of the prochiral radical anion, resulting from single-electron reduction of a *N*-sulfonylaldimine, and a chiral aminophosphonium ion (**24**). Here, chiral ion **24** governs the enantiofacial approach of the oxidatively generated *N*-aryl α-amino radical. While previous work from our laboratory demonstrated that asymmetric radical–radical coupling reactions were viable (see Scheme 10),[51] the protocol outlined in Scheme 11 represents the first example of an asymmetric radical–radical coupling reaction with useful levels of enantiocontrol (see Scheme 32d for another recent example). Challenging carbon–carbon bond-forming reactions between sterically congested C(sp³)–centers can also be achieved using radical–radical coupling platforms.[51,53,54] Indeed, the recent catalytic strategy outlined by Ooi[56] raises the exciting prospect of a general and enantioselective approach to these sterically encumbered systems.

Pioneering studies by the Knowles group have demonstrated the applicability of proton-coupled electron transfer (PCET) to organic synthesis through the development of a number of distinct catalytic transformations. Here, PCET-mediated radical generation can be accomplished under visible light irradiation using dual photoredox hydrogen bonding catalyst systems. Multisite PCET can be defined as the concomitant transfer of a proton and an electron to or from two independent donor/acceptor molecules.[57] The concerted nature of these events offers the opportunity to access radical species that would be kinetically inaccessible via sequential proton and electron transfer steps. In addition, the Knowles group have demonstrated that, through modulation of the properties of the separate proton and electron donor/acceptor catalysts, mild conditions can be used to effect selective homolytic cleavage of strong bonds in the presence of much weaker bonds.

In a seminal publication from Knowles, the development of ketyl radical cyclizations was reported based on a reductive PCET manifold, wherein aryl ketones could be reduced to the corresponding ketyl radical through the cooperative action of a photoredox catalyst and a phosphate H-bond donor (Scheme 12). The ketyl intermediate (i.e., **25**) can subsequently cyclize onto a pendant electron-deficient olefin to give an α-acyl radical, which can then abstract a hydrogen atom from 2-phenyldihydrobenzothaizoline (BT) to furnish the cyclized product (Scheme 12a).[58] In a subsequent report, Knowles and co-workers demonstrated that this net-reductive strategy could be used to effect an asymmetric intramolecular aza-pinacol
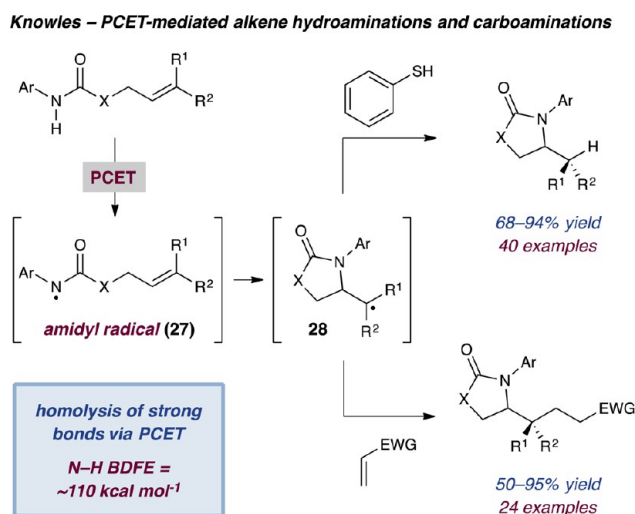
Scheme 12. Dual Photoredox Hydrogen Bonding Catalysis for Ketyl Olefin Cyclizations

(a) *Knowles – PCET-mediated ketyl-olefin cyclizations*

2 mol% [Ru(bpy)₃](BArF)₂
5 mol% (PhO)₂PO₂H

BT, THF, 26 W CFL

ketone/alkene

64–96% yield
1.2:1 to 16:1 dr

ketyl intermediate

25

BT   **26**

(b) *Knowles – Enantioselective aza-pinacol cyclizations*

10 mol% **26**
2 mol% [Ir(ppy)₂(dtbbpy)]PF₆

Hantzsch dihydropyridine,
1,4-dioxane, blue LEDs

ketone/hydrazone

45–96% yield
83–95% ee

reaction through the use of chiral phosphoric acid catalyst **26** (Scheme 12b). To achieve asymmetric induction, chiral catalyst **26** must remain tightly associated with ketyl radical **25** during the key carbon–carbon bond-forming step. Indeed, under the conditions outlined in Scheme 12b, the cyclic 1,2-amino alcohol products were generated in an efficient and highly enantioselective manner.[59]

In a further demonstration of the utility of PCET, the Knowles group has shown that amidyl radicals can be oxidatively generated from the corresponding amides through the homolytic cleavage of the strong N–H bond (BDFE = 110 kcal mol⁻¹) (Scheme 13). The highly electrophilic amidyl radical (**27**) can then cyclize onto a pendant alkene to generate a new nucleophilic C-centered radical (**28**). This radical can then either be trapped by a Michael acceptor, yielding the

Scheme 13. Dual Photoredox Hydrogen Bonding Catalysis for Amidyl Radical Cyclization Reactions via PCET

Knowles – PCET-mediated alkene hydroaminations and carboaminations

PCET

amidyl radical (**27**)

28

68–94% yield
40 examples

homolysis of strong bonds via PCET

N–H BDFE =
~110 kcal mol⁻¹

50–95% yield
24 examples

product of net carboamination of the alkene,[60] or undergo a hydrogen atom transfer event with thiophenol, thereby furnishing the hydroamination product.[61]

■ DUAL PHOTOREDOX ORGANOCATALYSIS: HYDROGEN ATOM TRANSFER

Hydrogen atom transfer (HAT) has been of long-standing interest in organic free radical chemistry.[62] Several groups have exploited HAT catalysts for the development of synthetically valuable photoredox-catalyzed transformations. In general, electron transfer between a photocatalyst and an organic substrate generates a reactive open-shell intermediate, which after participating in the desired chemistry must be converted back to a closed-shell species. In the absence of an additional catalyst, this second electron transfer event can be challenging. Seminal work from the Nicewicz group demonstrated that open-shell intermediates, which do not readily interact with the photocatalyst directly, could be converted to closed-shell products via hydrogen atom transfer with 2-phenylmalonitrile. In their initial report, hydroetherification of alkenols was achieved using a dual photoredox HAT strategy.[63] Here, organic dye 9-mesityl-10-methylacridinium perchlorate ([Mes-Acr]ClO₄), which possesses a highly oxidizing excited state (**29**), undergoes single-electron transfer with alkene **31** to deliver the corresponding radical cation **32** (Scheme 14). This highly electrophilic species is then primed to intercept a wide range of nucleophiles, and in the case of alcohol-tethered radical cation **32**, radical **33** is generated. Reduction of the carbon-centered radical (**33**) with photocatalyst **30** cannot readily occur, and as such, the reaction proceeds with low efficiency. However, when an additional single-electron redox mediator such as catalyst **34** is present, radical **33** can undergo a HAT event to deliver the tetrahydrofuran product. Moreover, the 2-phenylmalonitrile radical (**35**) formed during this process can be readily reduced by photocatalyst **30**, thereby closing the photoredox cycle and generating anion **36**. Finally, protonation of **36** regenerates the HAT catalyst (**34**) and closes the organocatalytic cycle. Notably, intramolecular cyclization of the pendant alcohol yields the product of anti-Markovnikov hydroetherification, a challenging transformation using traditional organic methods.

The Nicewicz group has subsequently extended this photoredox HAT strategy to enable the development of a range of alkene functionalization protocols using either 2-phenylmalonitrile or thiophenol derivatives as the HAT catalyst, in conjunction with the aforementioned mesityl acridinium photocatalyst. In many cases, thiophenol catalysts proved superior due to the faster rate of HAT between carbon-centered radicals and thiols. As shown in Scheme 14, these transformations include intermolecular hydroacetoxylation,[64] intra- and intermolecular hydroamination,[65] a range of novel polar radical crossover cycloadditions,[66] as well as a method for the direct anti-Markovnikov addition of mineral acids to styrenes.[67]

Nicewicz has also utilized this catalytic strategy, wherein a HAT event returns open-shell intermediates to a closed-shell species, in several mechanistically distinct transformations. Following on from earlier work from Fukuzumi and co-workers on the photocatalytic C–H fluorination and oxygenation of arene C–H bonds,[68] Nicewicz reported a protocol for the oxidative amination of C–H bonds of electron-rich arenes using catalytic TEMPO as the HAT catalyst with oxygen as the terminal oxidant (Scheme 15).[69] Here, oxidation of the

Scheme 14. Dual Photoredox HAT Catalysis for the Generation and Trapping for Alkene Radical Cations
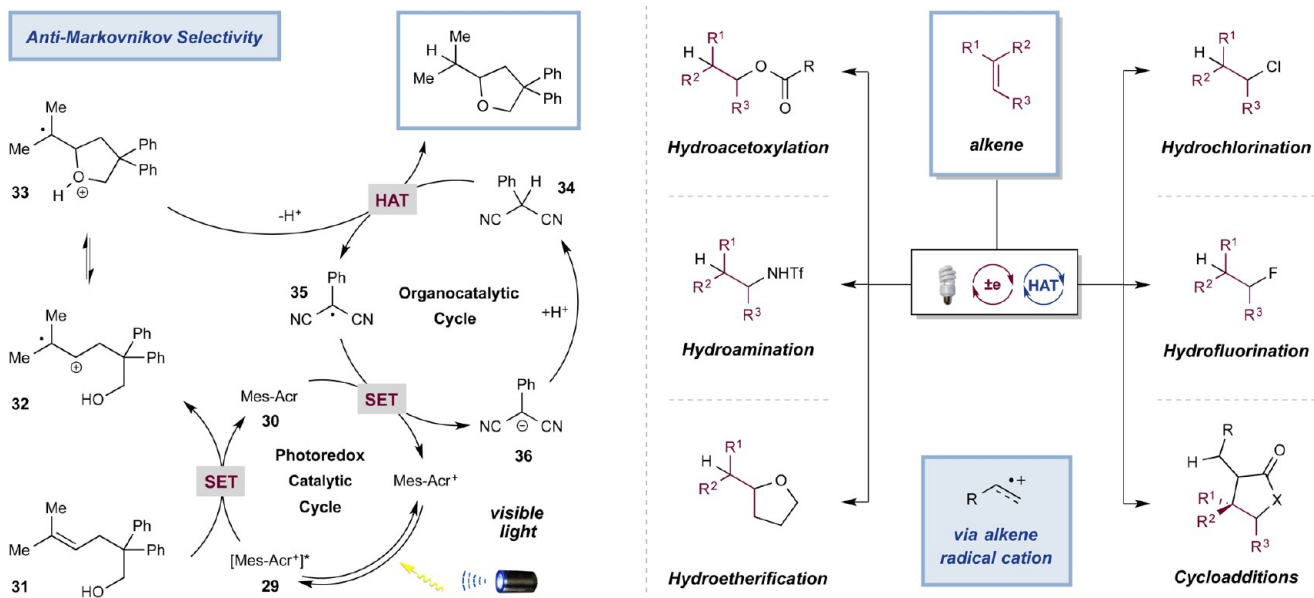
Scheme 15. Oxidative Amination of Electron-Rich Arenes via Dual Photoredox HAT Catalysis
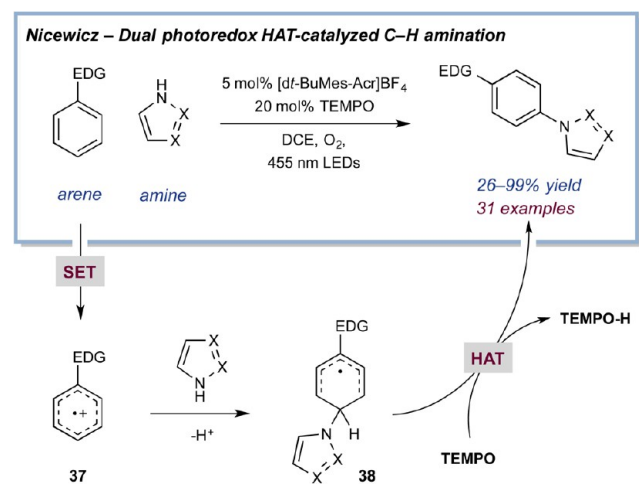
electron-rich arene delivers electrophilic radical cation **37**, and this reactive intermediate can be subsequently trapped with an amine nucleophile to generate a neutral radical (**38**). Finally, HAT between this open-shell species and TEMPO reestablishes aromaticity to deliver the aminated product. Regeneration of TEMPO from TEMPO−H is proposed to occur via a HAT event with superoxide, and accordingly, oxygen is the terminal oxidant that mediates regeneration of the photocatalyst.

Inspired by early work from the Akita and König groups demonstrating photoredox-mediated oxytrifluoromethylation and arylation of electron-rich alkenes,[70] the Gouverneur[71] and Nicewicz[72] groups independently reported methods for hydrotrifluoromethylation of alkenes. In both of these reports, addition of trifluoromethyl radical to the alkene is followed by a HAT event to furnish the trifluoromethylated products. In the report by Gouverneur and co-workers, the trifluoromethyl radical is generated by reduction of Umemoto's reagent and, upon addition to the alkene, the resulting C-centered radical undergoes a HAT event with methanol, the reaction solvent

(Scheme 16a). In the Nicewicz report, the trifluoromethyl radical is generated by single-electron oxidation of Langlois's reagent. Here, stoichiometric thiophenol (for styrenes) or catalytic methyl thiosalicylate (for aliphatic alkenes) were employed as HAT catalysts. In this latter case it is postulated that HAT from the trifluoroethanol (TFE) medium may also be occurring as low turnovers were observed in the absence of TFE (Scheme 16b).

Our laboratory has developed a photoredox HAT catalysis platform, wherein light-mediated generation of radical HAT catalysts (first described by Roberts and co-workers using conventional radical generation protocols)[73] enables functionalization of a wide range of C−H bonds. In 2014, we reported that a thiol catalyst, methyl thioglycolate (**39**), could be used to active the C−H bonds of benzylic ethers when in the presence of a photoredox catalyst and visible light. Generation of the active thiyl radical HAT catalyst (**40**) could occur via PCET from the parent thiol (**39**), or alternatively, deprotonation to the thiolate could be followed by a separate oxidation event. The thiyl radical (**40**) can readily abstract hydrogen atoms from benzylic ethers to generate the corresponding C-centered

Scheme 16. Dual Photoredox HAT-Catalyzed Hydrotrifluoromethylation
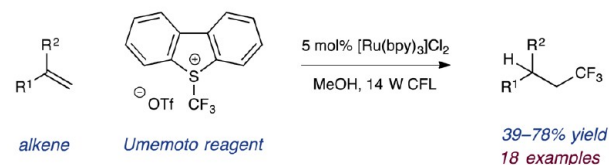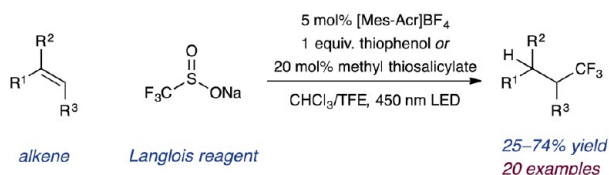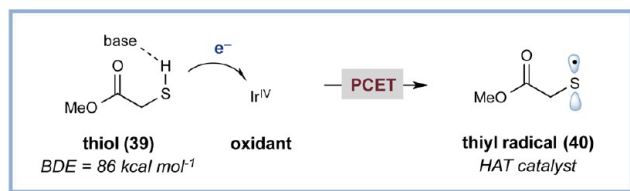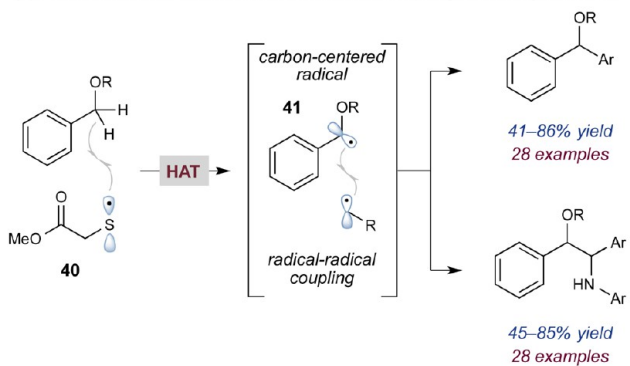
radical (**41**). In our initial report, we demonstrated that radical **41** could subsequently engage in a radical−radical coupling event with the reduced form of electron-deficient cyanoarenes to deliver benzhydryl ethers (Scheme 17a).[74] We have subsequently expanded this catalytic strategy to the development of intermolecular aza-pinacol reactions wherein the transient benzylic radical **41** is coupled with a persistent α-amino radical, generated via single-electron reduction of an imine, to furnish vicinal amino ether products.[75] This strategy is complementary to the previously discussed radical−radical α-arylation of amines (see Scheme 5) as, in this scenario, oxidation of the HAT catalyst rather than the substrate is required. As a result, HAT catalysis enables direct functionalization of substrates that are not readily oxidized by typical photoredox catalysts. Moreover, by modification of the thiol catalyst, we have shown this strategy can also be applied to the functionalization of allylic C−H bonds (Scheme 17b).[76]

By employing a similar photoredox HAT strategy, we have developed a protocol for the direct alkylation of heteroarenes using simple alcohols as the alkylating agent (Scheme 18a).[77] Thiyl radical **43**, generated by oxidation of a thiolate or PCET from thiol **42**, can abstract a hydrogen atom from alcohol **44** to generate an α-hydroxy radical (**45**). This highly nucleophilic radical (**45**) can then add to protonated heteroarenes (**46**) in an analogous fashion to the classic Minisci reaction.[78] The resultant open-shell species (**47**) is then deprotonated and subsequently undergoes spin-center shift (SCS) to cleave the C−O bond and eliminate water. Finally, electrophilic radical **48** can be reduced by the excited photocatalyst and protonated to furnish the alkylated heteroarene. Inspiration for the design of the ke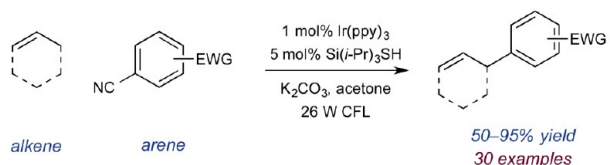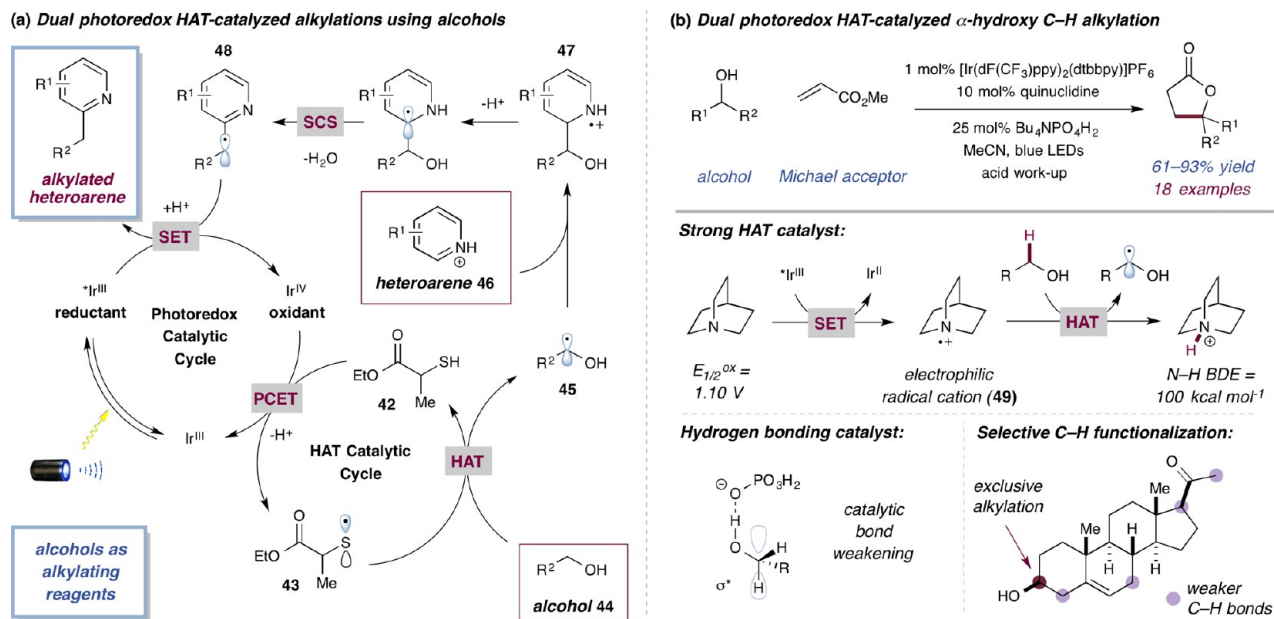y spin-center shift step in this alkylation protocol was taken from a commonly occurring biological phenomenon wherein conversion of ribose to deoxyribose, a vital step in DNA biosynthesis, occurs via an analogous radical-mediated elimination event.[79]

As a result of our long-standing interest in the exploitation of native functionality as a handle for synthetic elaboration, we have recently focused on examining HAT catalysts that have the capacity to activate strong C−H bonds. To this end, bicyclic tertiary amines such as quinuclidine have been examined as the N−H bond formed during the HAT event is considerably stronger than the S−H bond of the previously discussed thiol catalysts.[80] By leveraging photoredox, HAT, and hydrogen bonding catalysis, our laboratory has successfully developed a strategy for the selective alkylation of α-hydroxy C−H bonds with Michael acceptors (Scheme 18b).[81] In this protocol, both a quinuclidine HAT catalyst and a phosphate hydrogen bonding catalyst are required in order to achieve selective functionalization of α-hydroxy C−H bonds over other weaker C−H bonds. Here, a hydrogen bonding interaction between the phosphate and the alcohol induces a drastic weakening of the α-hydroxy C−H bonds and, in addition, increases the hydricity of the C−H bonds.[82] As a result, the highly electrophilic radical cation (**49**), formed via oxidation of quinuclidine, can readily abstract an activated α-hydroxy C−H bond. The resultant α-hydroxy radical is highly nucleophilic and is readily trapped by electron-deficient alkenes to ultimately deliver functionalized butyrolactone products (upon lactonization of the alkylated alcohol). The outlined bond-weakening strategy enables selective alkylation of α-hydroxy C−H bonds in the presence of much weaker C−H bonds, such as allylic and α-acyl C−H bonds. The protocols outlined in this section highlight that photoredox catalysis can be used in concert with both covalent and noncovalent organocatalytic activation modes to achieve previously elusive synthetic transformations. In addition, highly enantioselective protocols have been developed using these approaches despite the anticipated difficulty of rendering radical reactions stereoselective due to elongated bonds in the transition state. Moreover, we propose that by exploiting noncovalent interactions, highly selective methods for the activation of native functionality, such as simple C−H bonds, in complex molecular settings are likely to be achievable, thereby facilitating the development of methods for late-stage functionalization.

METALLAPHOTOREDOX CATALYSIS

The wealth of synthetic transformations developed through the combination of photoredox catalysis and organocatalysis demonstrates the powerful nature of dual catalytic methods, whereby the unique reactivity of different activation modes can be harnessed to enable novel bond disconnections. In this regard, a new catalysis platform has recently emerged which combines photoredox catalysis with transition metal catalysis. This rapidly developing subfield, which is now termed "metallaphotoredox catalysis", further highlights the breadth of distinct reaction manifolds that can be accessed via multicatalytic strategies. It is not an overstatement to say that the field of organic chemistry has been revolutionized over the last half century by the development of metal-mediated cross-coupling technologies, and many of the resulting transformations have become indispensible to organic chemists.[83] Considering the importance of transition metal catalysis, it is perhaps unsurprising that metallaphotoredox catalysis, which allows access to distinct organometallic mechanistic pathways,

Scheme 17. Photoredox HAT-Mediated Functionalization of Allylic and Benzylic C−H Bonds

(a) *Photoredox HAT-mediated radical-radical couplings of benzylic ethers*

41–86% yield
28 examples

45–85% yield
28 examples

(b) *Photoredox HAT-mediated allylic arylations*

50–95% yield
30 examples

Scheme 18. Dual Photoredox HAT Methodologies Involving Activation of α-Hydroxy C−H Bonds

(a) *Dual photoredox HAT-catalyzed alkylations using alcohols*

(b) *Dual photoredox HAT-catalyzed α-hydroxy C−H alkylation*

has gained such considerable attention. Indeed, since an early report by Sanford in 2011,[84] there have been over 50 publications combining photoredox catalysis with transition metal catalysis. Herein, we will discuss key catalytic methodologies which demonstrate how this approach can facilitate disfavored reaction pathways, with particular emphasis on transformations where challenging C−C and C−X bond disconnections are accomplished.

The diverse reactivity of transition metal catalysts stems from their propensity to occupy various oxidation states and this critical feature enables them to interact with a broad array of coupling partners. In most cases, transition metal-catalyzed reactions proceed through a series of two-electron redox events (i.e., M^n to M^{n+2}).[85] However, recent advances combining photoredox catalysis with this reaction manifold has enabled facile single-electron modulation of catalyst oxidation states. Using this approach, reactive high-valent catalyst species can be formed thereby enhancing the rate of subsequent mechanistic steps (e.g., reductive elimination, vide infra) or increasing the reactivity of the catalyst toward a particular coupling partner (e.g., see Scheme 20). In addition, manipulation of the oxidation state can facilitate regeneration of the active catalyst, thereby enabling catalytic turnover. Photoredox catalysts can modulate the oxidation state of transition metal catalysts via a number of different mechanisms, such as by (i) a direct single-electron transfer event between the catalysts, (ii) oxidative/reductive generation of a radical coupling partner which can intercept the transition metal, or (iii) oxidative/reductive generation of a radical species which can undergo SET with the metal catalyst. Methodologies that proceed via either one or a combination of these mechanistic pathways are discussed in the subsequent sections.

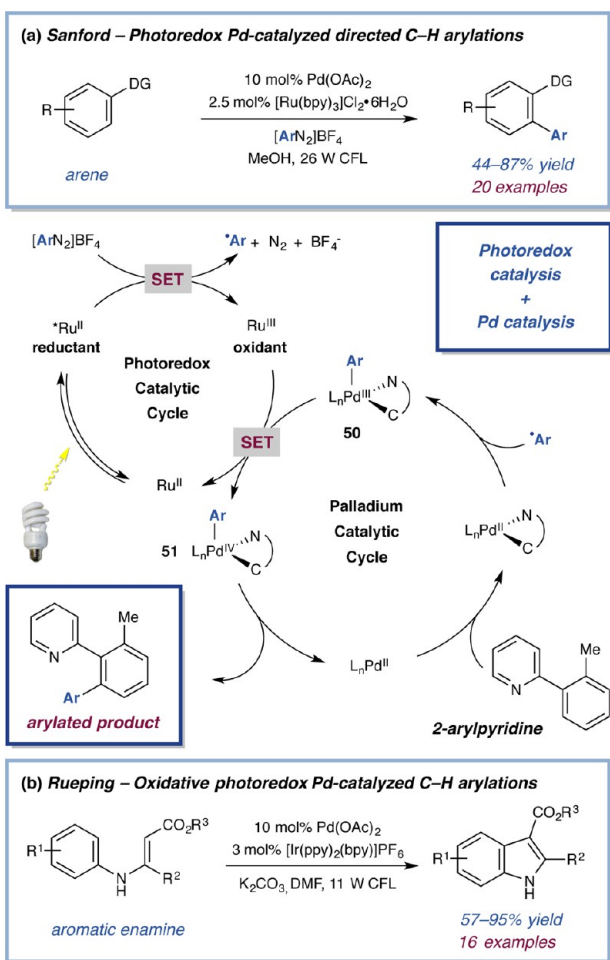## METALLAPHOTOREDOX CATALYSIS: C−C BOND FORMATION

The first example of photoredox catalysis being used in conjunction with transition metal catalysis was reported by Osawa in 2007.[86] Here, the efficiency of Pd-catalyzed Sonogashira reactions was shown to significantly increase in

the presence of $[Ru(bpy)_3](PF_6)_2$ and visible light. The role of the photocatalyst was not elucidated and, consequently, the significance of combining photoredox and transition metal catalysis was not fully appreciated until the seminal report of Sanford and co-workers four years later. In this latter study, directed C−H arylations using aryldiazonium salts were accomplished by employing a dual photoredox Pd catalyst system under irradiation with a household visible light source (Scheme 19a).[84,87] In the proposed mechanism, the photocatalyst is implicated in two key steps: (i) reduction of the aryldiazonium salt to generate an aryl radical and (ii) oxidation of the Pd(III)−aryl species (**50**) via a direct SET event. Together, these two steps facilitate the generation of Pd(IV)−aryl species **51** which can undergo reductive elimination to deliver the biaryl products.[88] Previous Pd-catalyzed C−H arylation protocols required elevated temperatures (~100 °C);[89] however, under the outlined dual photoredox Pd catalysis conditions, C−H arylation proceeded in an efficient manner at ambient temperature.

Rueping and co-workers exploited this reactivity in the development of Pd-catalyzed intramolecular C−H olefinations which, in the absence of previously required superstoichiometric strong oxidants, delivered indoles from aromatic enamines (Scheme 19b).[90] Here, the photocatalyst is proposed to facilitate reoxidation of the generated Pd(0) catalyst by either direct SET or through reductive generation of superoxide. Subsequently, Rueping demonstrated that photoredox catalysis could also aid Ru- and Rh-catalyzed oxidative Heck reactions in a mechanistically analogous manner.[91,92]

Inspired by the work of Sanford, the Glorius and Toste laboratories have demonstrated that light-mediated generation of aryl radicals from aryldiazonium salts could also be harnessed in dual photoredox Au-catalyzed protocols to accomplish oxy-/amino-arylation of alkenes and arylative ring expansions, respectively (Scheme 20).[93,94] Experimental and computational mechanistic studies support the generation of cationic Au(III)−aryl species **52**, which can then engage the alkene to ultimately deliver the arylated products.[94,95] As illustrated in Scheme 20c, this strategy has been extended to arylative Meyer−Schuster

**Scheme 19. Dual Photoredox Pd Catalysis for C−H Arylation**

(a) *Sanford – Photoredox Pd-catalyzed directed C−H arylations*

arene

10 mol% Pd(OAc)$_2$
2.5 mol% [Ru(bpy)$_3$]Cl$_2$·6H$_2$O

[ArN$_2$]BF$_4$
MeOH, 26 W CFL

44–87% yield
20 examples

[ArN$_2$]BF$_4$ → SET → •Ar + N$_2$ + BF$_4^-$

*Ru^{II} reductant / Ru^{III} oxidant

Photoredox Catalytic Cycle

Ru^{II}

SET

Photoredox catalysis + Pd catalysis

L$_n$Pd^{III} **50**
51 L$_n$Pd^{IV}

Palladium Catalytic Cycle

L$_n$Pd^{II}

arylated product

2-arylpyridine

(b) *Rueping – Oxidative photoredox Pd-catalyzed C−H arylations*

aromatic enamine

10 mol% Pd(OAc)$_2$
3 mol% [Ir(ppy)$_2$(bpy)]PF$_6$

K$_2$CO$_3$, DMF, 11 W CFL

57–95% yield
16 examples

Scheme 20. Dual Photoredox Au-Catalyzed Methodologies

(a) *Glorius – Photoredox Au-catalyzed oxy- and amino- arylation of alkenes*

alkene   aryldiazonium

10 mol% [Ph$_3$PAu]NTf$_2$
2.5 mol% [Ru(bpy)$_3$](PF$_6$)$_2$

MeOH, 23 W CFL

32–83% yield
18 examples

(b) *Toste – Photoredox Au-catalyzed ring expansion-arylation reactions*

alkene   aryldiazonium

10 mol% Ph$_3$PAuCl
2.5 mol% [Ru(bpy)$_3$](PF$_6$)$_2$

MeOH/MeCN (3:1), 32 W CFL

32–90% yield
21 examples

(c) *Photoredox Au-catalyzed methodologies*

[L$_n$−Au^I−X]

[Ru]
[ArN$_2$]BF$_4$

[L$_n$−Au^{III}−X]$^+$ Ar **52**

photoredox-mediated generation of reactive Au(III)-aryl species

Shin (2016)
Glorius (2016)

Toste (2016)
Glorius (2016)

Glorius (2016)

Toste (2015)

Scheme 21. Dual Photoredox Cu-Catalyzed Trifluoromethylation of Boronic Acids

Sanford – Trifluoromethylation of boronic acids

boronic acid

20 mol% CuOAc
1 mol% [Ru(bpy)$_3$]Cl$_2$·6H$_2$O

CF$_3$I, K$_2$CO$_3$
DMF, 60 °C, 26 W CFL

39–93% yield
22 examples

B(OH)$_2$(X)

F$_3$C−Cu^{III}X

cross-coupled product

B(OH)$_2$

F$_3$C−Cu^{III}X$_2$

Copper Catalytic Cycle

Cu^{I}X

boronic acid **53**

Cu^{II}X$_2$

SET / *Ru^{II} oxidant (14)

•CF$_3$

Photoredox Catalytic Cycle

Ru^I
reductant (15)

Ru^{II} **13**

Photoredox catalysis + Cu catalysis

SET

•CF$_3$ + I$^-$ CF$_3$I

---

rearrangements,[96] C(sp)−C(sp^2) couplings,[97] arylative hydrations of alkynes,[96b] and the synthesis of aryl phosphonates.[98] Photoredox-mediated in situ generation of reactive Au(III) complex **52** both facilitates the subsequent substrate activation/ rearrangement steps and, perhaps more importantly, allows protodeauration termination, a more commonly observed pathway for Au(I)- or Au(III)-mediated reactions, to be replaced with a terminal aryl−C reductive elimination step.[99]

In 2012, Sanford demonstrated that photoredox catalysis could also be combined with Cu catalysis, and through the development of this dual catalytic system, efficient trifluoromethylation of boronic acids was achieved (Scheme 21).[100] The ability to install trifluoromethyl groups into complex molecules in a facile and selective manner is widely recognized as an important goal for synthetic chemists due to the favorable properties that these groups can impart to medicinally relevant compounds.[101] In pursuit of this goal, our laboratory demonstrated that generation of •CF$_3$ from CF$_3$I could be achieved under mild conditions through the use of photoredox catalysis.[42] Sanford elegantly utilized this photoredox-mediated method for the generation of •CF$_3$ in the dual photoredox Cu-catalyzed trifluoromethylation protocol outlined in Scheme 21. Here, generation of Cu(III)−CF$_3$ complex **53** from Cu(I) occurs via a direct SET event with photoexcited [Ru(bpy)$_3$]$^{2+}$ (**14**) followed by capture of the reductively generated •CF$_3$. Subsequent transmetalation of the aryl group from the boronic
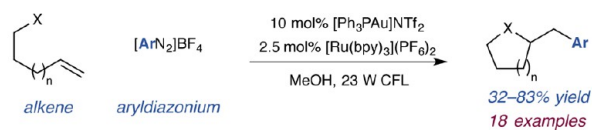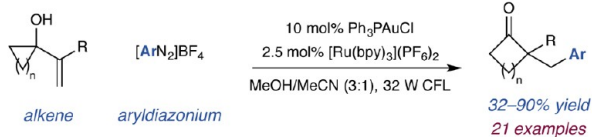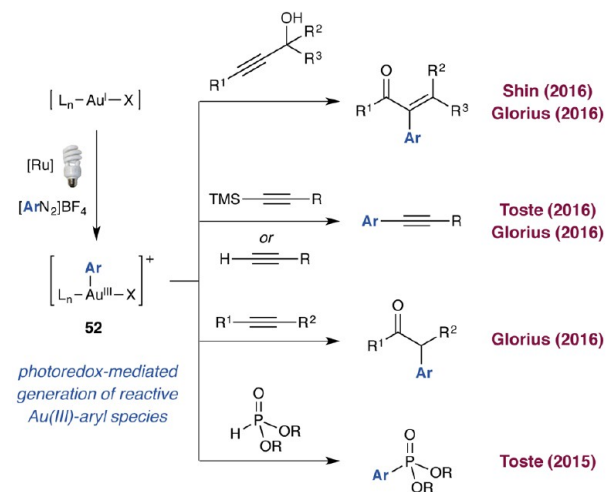
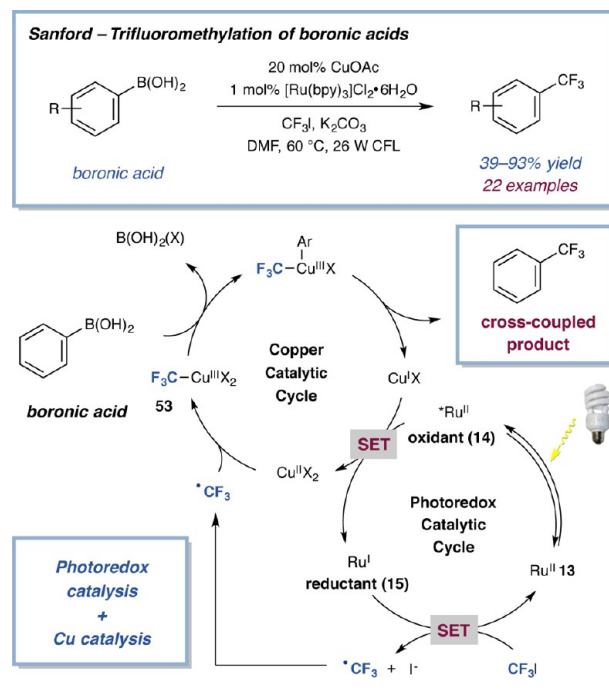acid and reductive elimination delivers the desired trifluoromethylated products. Notably, the use of fluoroalkyl iodides as

Scheme 22. Dual Photoredox Ni-Catalyzed Cross-Couplings Using Various Oxidizable Radical Precursors
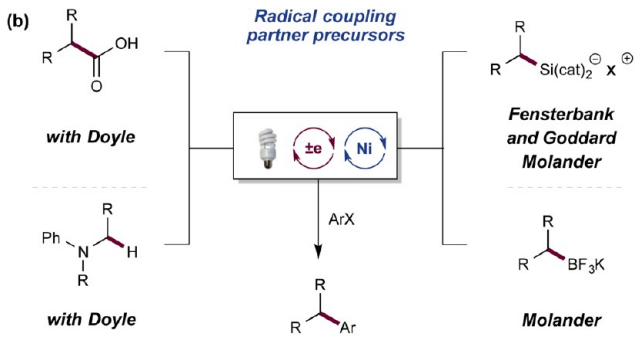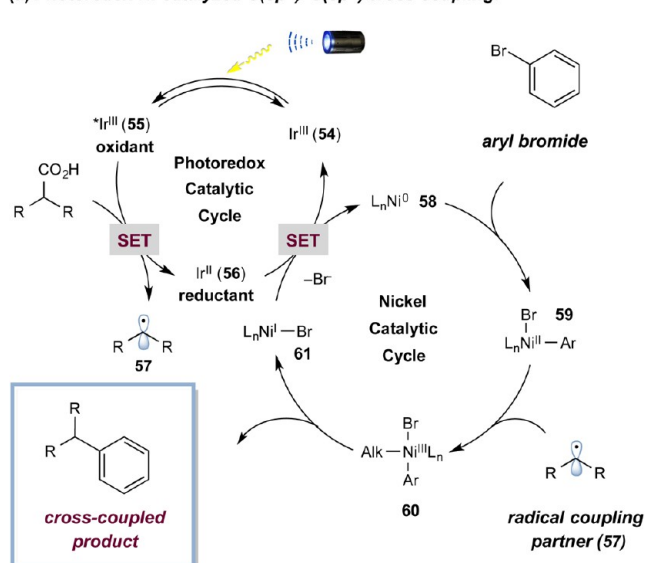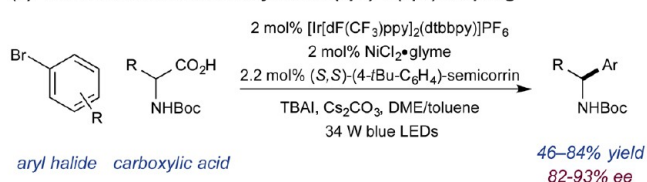
the radical source enables functionalization with a variety of long-chain perfluoroalkanes.

Our laboratory has long been interested in the concept of "switching on" a broad array of reaction pathways which are either inaccessible or present a significant challenge using conventional transition metal catalysis. In this regard, we recently focused our efforts on the merger of photoredox and Ni catalysis, cognizant that nickel may occupy a privileged position (vs second-row transition metals) due to its ability to readily undergo one-electron oxidation state changes.[85c,102] The realization of this dual catalysis strategy was reported concomitantly by the Molander group and the Doyle group in collaboration with our own lab.[103,104] While using different radical precursors, both of these reports stem from development of the general catalysis platform outlined in Scheme 22a. Here, it was postulated that oxidation of the radical precursor (e.g., a carboxylic acid) by excited Ir(III) photocatalyst **55** facilitates generation of a nucleophilic radical coupling partner (**57**). Simultaneously, oxidative addition of a Ni(0) catalyst (**58**) into the aryl bromide generates Ni(II)–aryl species **59**, which can intercept the C-centered radical, thereby accessing Ni(III) complex **60**.[105] At this stage, reductive elimination delivers the cross-coupled product, and subsequent SET from Ir(II) species **56** to Ni(I) complex **61** closes both catalytic cycles. While elegant work from the Weix group has demonstrated that the addition of alkyl radicals to analogous Ni(II)–aryl species can be used to accomplish reductive cross-electrophile coupling,[106] the strategy outlined in Scheme 22 offers a complementary, redox-neutral approach which, in turn, facilitates the use of nontraditional cross-coupling reaction partners.

A key aspect of our design plan was the use of carboxylic acids as the nucleophilic coupling partner. As previously discussed, decarboxylative generation of C-centered radicals has found widespread utility in photoredox-mediated technologies (see Scheme 7), and it was anticipated that interfacing this activation mode with transition metal cross-coupling would significantly expand the utility of this reaction platform. Indeed, by employing carboxylic acids in the outlined photoredox Ni dual catalysis manifold we have shown that these abundant,
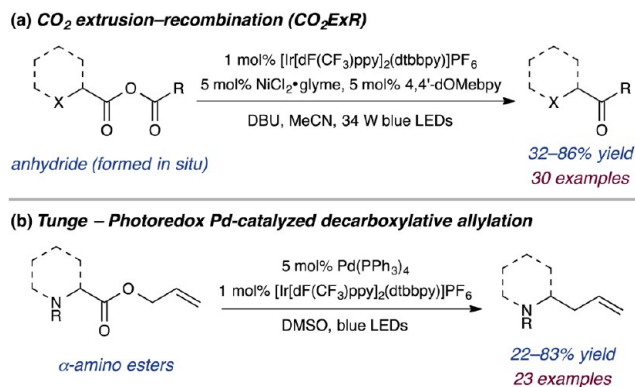
feedstock chemicals can be used in lieu of more traditional, prefunctionalized organometallic coupling partners. Considerable research efforts from Goößen and others have focused on the development of decarboxylative transition metal-catalyzed protocols, and although significant advances have been made, the majority of these methodologies have focused on the utilization of aryl carboxylic acids.[107] As previously discussed (see Scheme 1c), photoredox-mediated decarboxylations to generate C-centered radicals have been reported by the groups of Okada[12,13] and Overman[108] using redox-active, carboxylic acid derived N-(acyloxy)phthalimides via a complementary net reductive strategy. We were pleased to note that the value of our decarboxylative-nickel cross-coupling strategy has not gone unrecognized. Indeed, the Baran and Weix laboratories have recently developed elegant variants using Okada's redox-active esters in combination with organozinc nucleophiles.[109] In addition to carboxylic acids, we have shown that α-amino C−H bonds of N-arylamines can be used as handles for cross-coupling in the outlined photoredox Ni catalysis methodology. Here, α-amino radicals are generated via an oxidation−deprotonation sequence (see Scheme 5). With respect to the concurrent publication from the Molander laboratory described above, trifluoroborates salts were chosen as nucleophilic coupling partners, a system that has a broad range of synthetic utility.

The number of cross-coupling protocols that have been rapidly developed based on this catalysis platform demonstrates the broad applicability of this metallaphotoredox strategy (Scheme 22). For example, Molander has demonstrated that, by using trifluoroborate salts as the radical precursor, coupling of benzylic,[110] secondary alkyl,[111] α-alkoxy,[112] and α-amino[113] radicals can be achieved. Interestingly, for benzylic trifluoroborate salts, only moderate levels of enantioselectivity were observed when a chiral ligand was employed and computational studies suggest that rapid dissociation of the benzylic radical from the Ni(III)−aryl species occurs, thereby rendering reductive elimination the enantiodetermining step. Recently, both the Molander group[114] and Fensterbank, Ollivier, and Goddard[115] demonstrated that alkylbis(catecholato)silicates could also be utilized as radical precursors in photoredox Ni-

catalyzed cross-couplings. While preformation of the silicates from the corresponding trimethoxysilanes is required, a notable feature of this methodology is the ability to couple unstabilized primary and secondary radicals in excellent yield. In addition, whereas other radical precursors require the presence of a base, these silicate derivatives undergo oxidation and generation of the C-centered radical under neutral or even mildly acidic conditions. As such, unprotected amines, a useful functional handle, can be incorporated directly using ammonium silicate precursors in this cross-coupling protocol. In a similar vein, our laboratory has demonstrated that dual photoredox Ni catalysis can enable decarboxylative arylations and vinylations of α-oxy, α-amino, and benzylic acids.[116] In collaboration with the Fu group, we have accomplished the decarboxylative arylation of α-amino acids with useful levels of enantioselectivity via the development of an appropriate chiral Ni catalyst system (Scheme 22c).[117] The generality of this photoredox-mediated strategy was exemplified by extending the scope to α-oxo acids whereby, upon decarboxylation, an acyl radical is generated. By combining this activation mode with Ni catalysis, aryl ketones could be generated in high yields.[118] It is worth noting that, following this publication, Fu and Shang demonstrated that aryl ketones could also be generated through the merger of photoredox catalysis with Pd catalysis and this transformation likely proceeds via a similar mechanistic pathway.[119] In addition, Wang and co-workers revealed that aryl ketones can be generated by combining photoredox-mediated acyl radical generation with directed Pd-catalyzed C–H activation.[120]

The utility of decarboxylative metallaphotoredox catalysis for intramolecular C–C bond-forming protocols was highlighted with the development of a CO_2 extrusion–recombination strategy. Here, oxidative addition adjacent to a carboxylate group can initiate intramolecular fragment couplings via a photoredox-mediated decarboxylation and recombination sequence. Using this design plan, we showed that anhydrides, generated in situ from carboxylic acids and acid chlorides, underwent extrusion of CO_2 to deliver aliphatic ketones (Scheme 23a).[121] Subsequently, dual photoredox Ni-mediated acylation of N-arylamines was demonstrated by the Doyle group using anhydrides or thioesters as the acyl donor.[122] Moreover, Tunge and co-workers reported a dual photoredox Pd catalyst system for the decarboxylative allylation of α-amino and α-phenyl allyl esters (Scheme 23b).[123] Mechanistic studies indicated that, after oxidative addition and decarboxylation, recombination can occur though radical–radical coupling

(upon reduction with the photocatalyst) or via a metal-mediated pathway. Interestingly, experimental observations suggested that the operative pathway is dependent on the extent of stabilization of the incipient radical. Decarboxylative allylation of N-arylamines using allyl phosphates was later reported by Xiao and Lu utilizing a similar metallaphotoredox strategy.[124]

An attractive feature of the outlined decarboxylative cross-coupling methodology is the capacity to use feedstock chemicals, such as amino acids, directly as coupling partners and without derivatization to specialized esters that require redox triggering. In this regard, we have endeavored to expand the repertoire of native functionality that can engage directly in cross-coupling. Through the development of a triple catalytic cross-coupling strategy combining photoredox, HAT, and nickel catalysis, we have demonstrated that $C(sp^3)$–H bonds can be used as latent nucleophiles (Scheme 24).[125] As shown previously, hydrogen atom transfer catalysis represents a powerful tool for direct C–H functionalization and, through judicious choice of HAT catalyst, strong bonds can be selectively targeted over weak bonds (see Scheme 18). Specifically, the use of 3-acetoxyquinuclidine (62), which generates a highly electrophilic radical cation (63) upon oxidation with an excited state photocatalyst, enabled the selective cross-coupling of hydridic C–H bonds to be achieved.

Scheme 24. Direct Functionalization of $C(sp^3)$–H Bonds through the Merger of Photoredox, HAT, and Ni Catalysis

Scheme 23. Metallaphotoredox-Catalyzed Intramolecular Decarboxylative Transformations
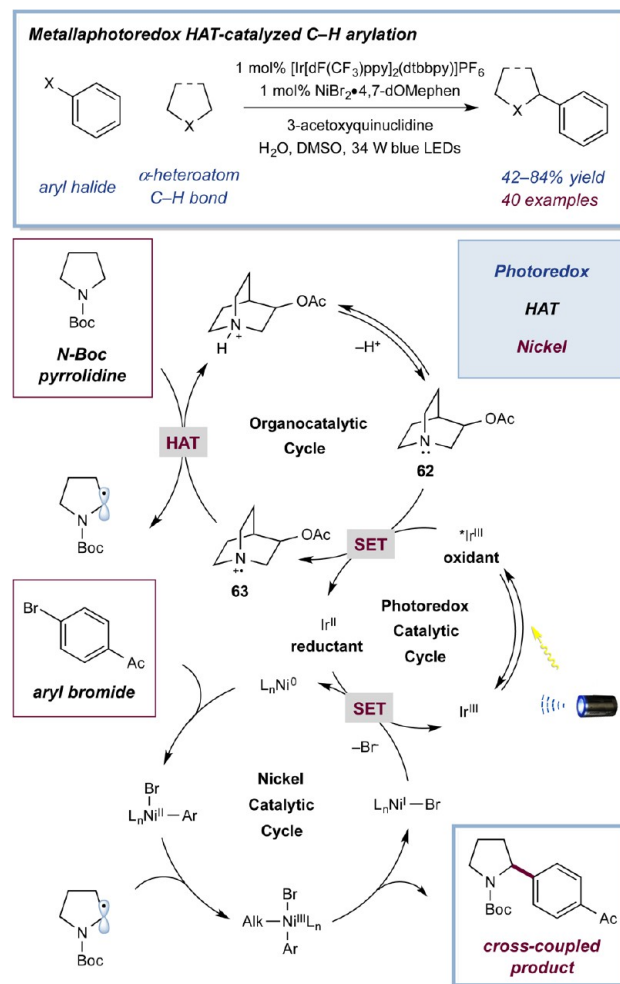
Under the conditions outlined in Scheme 24, direct arylation of a broad range of α-amino, α-oxy, and benzylic C–H bonds could be achieved. In this transformation, the photoredox catalyst both modulates the oxidation state of the Ni catalyst and mediates oxidation of amine 62 to radical cation 63, thereby controlling turnover of both catalytic cycles.

Recently, our laboratory has also exploited silyl radical-mediated halogen atom abstraction as a means to generate carbon-centered radicals from alkyl halides. The resultant radical can subsequently be utilized in nickel-catalyzed cross-couplings (Scheme 25).[126] This mechanistically distinct transformation proceeds via initial oxidation of bromide to bromine radical by the highly oxidizing excited state of an iridium photocatalyst (55). The electrophilic bromine radical is then primed to abstract a hydrogen atom from tris-(trimethylsilyl)silane (TTMSS). The resultant silyl radical can then abstract a halogen atom from the alkyl halide coupling partner, delivering a carbon-centered radical and generating a strong silicon–halogen bond in the process. The generated C-centered radical can then engage in nickel-catalyzed cross-couplings in a comparable manner to the other methodologies discussed in this section (vide supra).

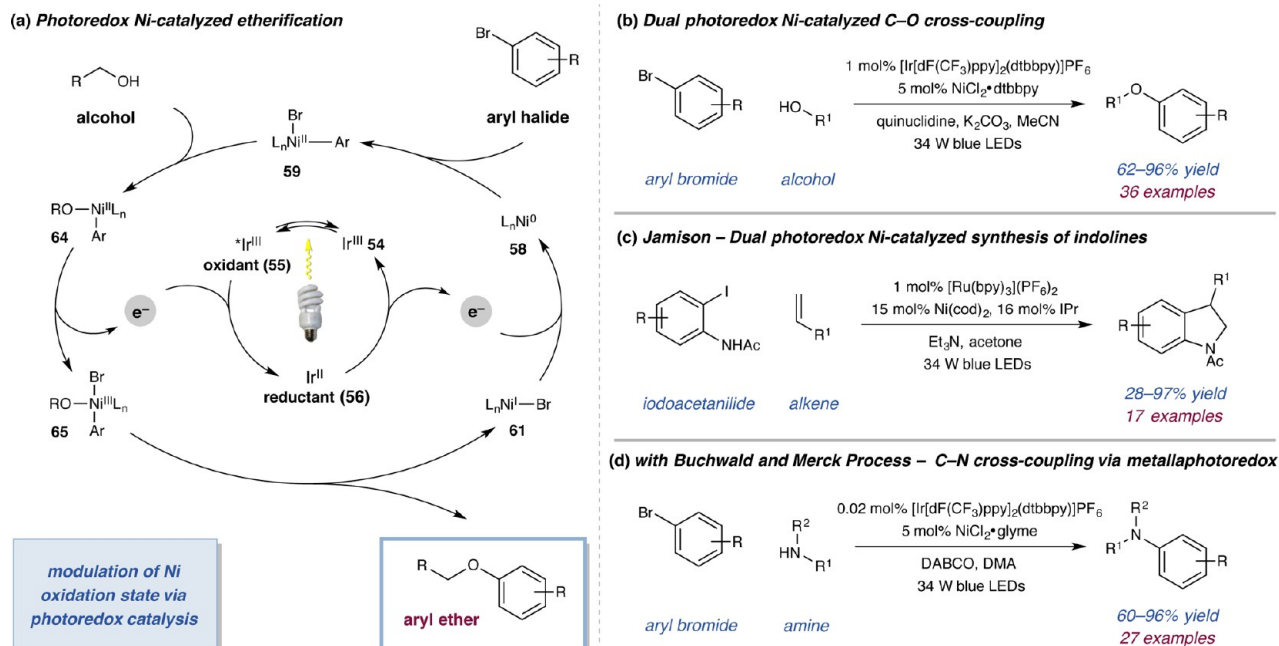**Scheme 25. Silyl Radical Activation of Alkyl Halides for Cross-Electrophile Couplings**
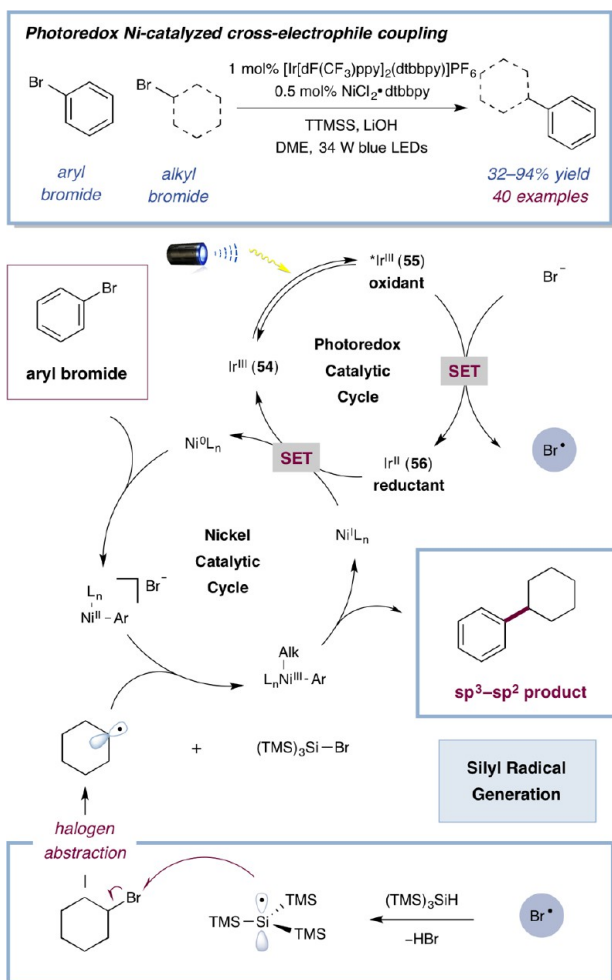
METALLAPHOTOREDOX CATALYSIS: C–X BOND FORMATION

A key feature of the C–C bond-forming methodologies outlined in the previous section is that, in general, the photocatalyst is responsible for both modulating the oxidation state of the transition metal catalyst and for (directly or indirectly) facilitating generation of a radical species that can intercept the metal. Recently, we questioned whether the photoredox catalyst could modulate the oxidation state of the transition metal alone and, in turn, provide entry to oxidation states that are not readily accessible under nonredox conditions. In turn, we anticipated that generating high valent metal species could facilitate kinetically unfavorable mechanistic pathways that are not currently viable under thermal control.

In order to test this general oxidation state modulation concept, we targeted a Ni-catalyzed etherification reaction. Both computational[127] and experimental studies[128] demonstrated that C–O bond formation from a Ni(II) species is thermodynamically "uphill". However, notably, Hillhouse and co-workers conducted stoichiometric studies which suggested that oxidation to a Ni(III) species enables reductive elimination to take place.[128] Indeed, in the presence of a photocatalyst and visible light, high efficiencies were observed for the coupling of aryl bromides with primary and secondary alcohols.[129] In the absence of light and/or photocatalyst, no product was observed, and the proposed mechanism for this transformation is outlined in Scheme 26a. Here, upon oxidative addition of the aryl halide and ligand exchange with the alcohol, Ni(II) species 64 is generated. At this stage, reductive elimination is disfavored. However, after oxidation by the excited Ir(III) photocatalyst (55), reductive elimination from Ni(III) complex 65 occurs in a facile manner to generate the C–O coupled product. The catalytic cycles are both closed via a SET event between photocatalyst 56 and Ni catalyst 61. This proposal was supported by mechanistic studies and the outlined transformation demonstrates the ability of photoredox catalysis to "switch on" inaccessible organometallic reaction pathways.

Using a similar rationale, the Jamison laboratory concurrently developed a dual photoredox Ni-mediated protocol for the synthesis of indolines from iodoacetanilides (Scheme 26c).[130] Under standard Ni-catalyzed conditions, low reactivity was observed and it was anticipated that C–N bond formation was the problematic step. In mechanistic studies similar to those conducted in our laboratory for the etherification reaction, it was observed that reductive elimination from stoichiometrically generated Ni(II) complexes only occurred upon exposure to an oxidant. More recently, in collaboration with the Buchwald laboratory and the Merck process division, our group has developed a general protocol for Ni-catalyzed C–N cross-couplings which, by employing a photocatalyst and visible light, proceed under mild conditions without the need for exogenous ligand or strong base (Scheme 26d).[131] The broad generality and high efficiency of Pd-catalyzed Buchwald–Hartwig reactions, arguably one of the most important cross-coupling methodologies, stems from the elegant design of ligands which destabilize the metal center, thereby facilitating C–N reductive elimination.[132] Utilizing metallaphotoredox catalysis, we have demonstrated a complementary destabilization strategy whereby modulation of the oxidation state of the nickel center allows Ni-catalyzed C–N couplings to proceed in a highly efficient manner, with broad substrate scope and without the requirement of ligand design or development.

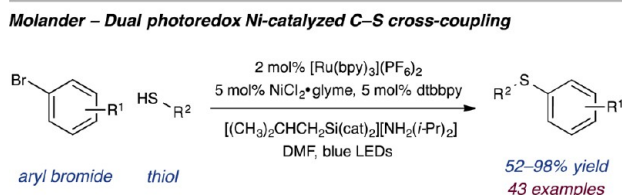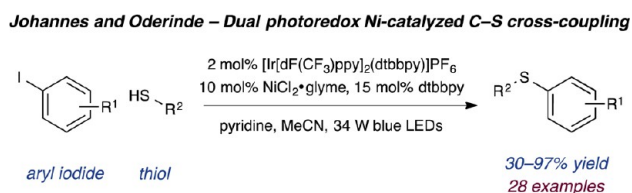**Scheme 26. Dual Photoredox Ni-Catalyzed C−O and C−N Cross-Couplings**

(a) *Photoredox Ni-catalyzed etherification*

modulation of Ni
oxidation state via
photoredox catalysis

aryl ether

(b) *Dual photoredox Ni-catalyzed C–O cross-coupling*

1 mol% [Ir[dF(CF₃)ppy]₂(dtbbpy)]PF₆
5 mol% NiCl₂•dtbbpy
quinuclidine, K₂CO₃, MeCN
34 W blue LEDs

aryl bromide   alcohol

62–96% yield
36 examples

(c) *Jamison – Dual photoredox Ni-catalyzed synthesis of indolines*

1 mol% [Ru(bpy)₃](PF₆)₂
15 mol% Ni(cod)₂, 16 mol% IPr
Et₃N, acetone
34 W blue LEDs

iodoacetanilide   alkene

28–97% yield
17 examples

(d) *with Buchwald and Merck Process – C–N cross-coupling via metallaphotoredox*

0.02 mol% [Ir[dF(CF₃)ppy]₂(dtbbpy)]PF₆
5 mol% NiCl₂•glyme
DABCO, DMA
34 W blue LEDs

aryl bromide   amine

60–96% yield
27 examples

In addition to Ni-catalyzed processes, reports by Kobayashi[133] and You and Cho[134] have demonstrated that both copper and palladium-catalyzed C−N couplings can benefit from combination with photoredox catalysis. In the former case, the efficiency and substrate scope of Cu-catalyzed Chan−Lam couplings were significantly improved by employing a photocatalyst and visible light. You and Cho demonstrated that dual photoredox Pd catalysis can facilitate the synthesis of carbazoles via a intramolecular C−H amination reaction. In both of these oxidative processes, it was postulated that the photocatalyst provides access to higher oxidation state metal complexes, Cu(III) and Pd(III)/Pd(IV) respectively, thereby enhancing the C−N bond-forming step.

Recently, both the Molander laboratory[135] and Johannes and Oderinde,[136] scientists at AstraZeneca described C−S coupling protocols that rely on the combination of photoredox and nickel catalysis (Scheme 27). In contrast to the C−N coupling studies by our laboratory and that of Jamison, these protocols are proposed to proceed via generation of a thiyl radical which can then intercept the nickel catalytic cycle (in a similar manner

to the C-centered radical in Scheme 22a). Johannes and Oderinde demonstrated that thiyl radicals could be generated through an oxidation-deprotonation sequence by using a sufficiently oxidizing Ir(III) photocatalyst and pyridine as base. In Molander's protocol, an alkylbis(catecholato)silicate was employed as the hydrogen atom abstractor. As discussed previously, oxidation of these silicates through SET with a photocatalyst generates C-centered radicals (see Scheme 22b), and in the C−S coupling protocol developed by Molander, the generated radical is proposed to undergo a HAT event with the thiol to deliver the required thiyl radical. Prior to these studies, Lu and Xiao showed that arylation of diarylphosphine oxides could be accomplished using a dual photoredox Ni catalyst system through in situ generation of a P-centered radical.[137]

In the oxidative C−N cross-coupling methodologies reported by the Kobayashi laboratory and You and Cho (vide supra), molecular oxygen is the terminal oxidant which facilitates turnover of the catalytic cycles.[133,134] Recently, Wu and Lei designed a dual photoredox cobalt catalyst system for the oxidative thiolation of C−H bonds that requires no external oxidant or proton acceptor and delivers hydrogen as the only byproduct (Scheme 28).[138] In the presence of a Ru(II) photocatalyst (**13**), a Co(II) catalyst and visible light, benzothiazoles were generated in high yields. The proposed mechanism involves initial photoexcitation of photocatalyst **13** to the oxidizing excited state **14** which can accept an electron from anion **70**, thereby generating S-centered radical **71**. Subsequent cyclization of radical **71** onto the pendant arene delivers **72**. Simultaneously, Ru(I) photocatalyst **15** undergoes SET with Co(III) complex **69** to regenerate Ru(II) catalyst **13** and afford Co(II) catalyst **66**. Complex **66** can then be further reduced by radical **72** to deliver Co(I) **67** and cation **73**. Finally, upon rearomatization of **73** to deliver the cyclized product, protonation of Co(I) **68** enables regeneration of Co(III) catalyst **69** with concomitant evolution of hydrogen. This strategy has also been applied to the C−H functionalization of N-arylamines and isochromans with β-keto esters.[139] While this catalysis mode is currently limited to substrates

Scheme 27. Dual Photoredox, Ni-Catalyzed C−S Cross-Coupling

Johannes and Oderinde – Dual photoredox Ni-catalyzed C–S cross-coupling

2 mol% [Ir[dF(CF₃)ppy]₂(dtbbpy)]PF₆
10 mol% NiCl₂•glyme, 15 mol% dtbbpy
pyridine, MeCN, 34 W blue LEDs

aryl iodide   thiol

30–97% yield
28 examples

Molander – Dual photoredox Ni-catalyzed C–S cross-coupling

2 mol% [Ru(bpy)₃](PF₆)₂
5 mol% NiCl₂•glyme, 5 mol% dtbbpy
[(CH₃)₂CHCH₂Si(cat)₂][NH₂(i-Pr)₂]
DMF, blue LEDs

aryl bromide   thiol

52–98% yield
43 examples

Scheme 28. Metallaphotoredox-Catalyzed Acceptorless Dehydrogenation for C−H Thiolation

Wu and Lei – C–H thiolation via dual photoredox Co catalysis

59–99% yield
14 examples
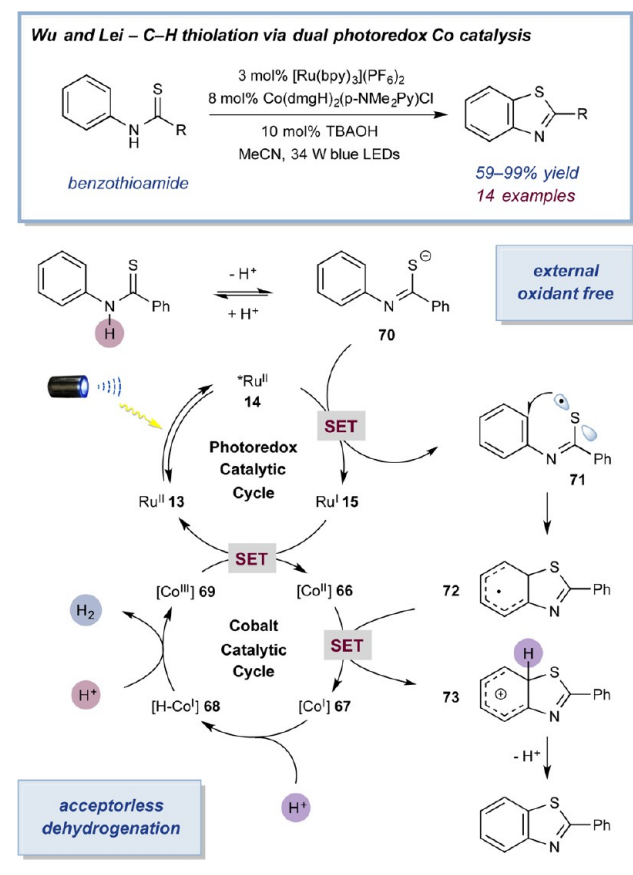
which can be oxidized by the photocatalyst, the extremely mild conditions under which acceptorless dehydrogenation can be achieved is notable.

The remarkable breadth of transformations outlined in this section, along with the rapid timeline of development, illustrates the powerful nature of metallaphotoredox catalysis. The interaction between photoredox catalysts and transition metal catalysts via single-electron transfer enables formerly inaccessible or challenging mechanistic pathways to be explored. There can be no question that this area will continue to grow at a dramatic pace over the next few years.

■ PHOTOREDOX LEWIS ACID CATALYSIS

Dual catalytic methods that combine light-mediated SET with a second mode of catalysis are synonymous with the growth of photoredox catalysis as a field in the modern era. Indeed, early reports from Yoon and our laboratory in 2008 demonstrated that photoredox could be successfully combined with Lewis acid catalysis and organocatalysis, respectively.[14,15] Since then, Yoon and others have sought to exploit the unique reactivity that can be accessed using dual photoredox Lewis acid catalysis. Importantly, these studies have demonstrated that Lewis acids that successfully function in these transformations can play a number of different roles. For example, coordination of the Lewis acid catalyst to a Lewis basic carbonyl or imine can facilitate reduction to the corresponding radical anion by decreasing the reduction potential of the π-system in question.[14] Moreover, the resultant radicals can also be stabilized by the Lewis acid catalyst, thereby suppressing back-electron transfer.[9c] Alternatively, the role of the Lewis acid catalyst can be independent from photoredox-mediated radical formation; for example, coordination to Lewis basic substrates has been shown to enhance the rate of nucleophilic radical addition in much the same manner that Lewis acids can facilitate two-electron conjugate additions (vide infra). A third possibility is that the Lewis acid catalyst interacts directly with the photocatalyst. In this regard, Lewis acid catalysts have been shown to stabilize reduced photocatalysts, thereby slowing down the rate of back-electron transfer.[140] Finally, coordination between the photocatalyst and the Lewis acid can also serve to modulate the redox properties of the photocatalyst excited state.[141]

Scheme 29. Dual Photoredox Lewis Acid-Catalyzed Cycloadditions

(a) *Dual photoredox Lewis acid-catalyzed [2+2] cycloadditions*

[2+2] cycloadduct (77)
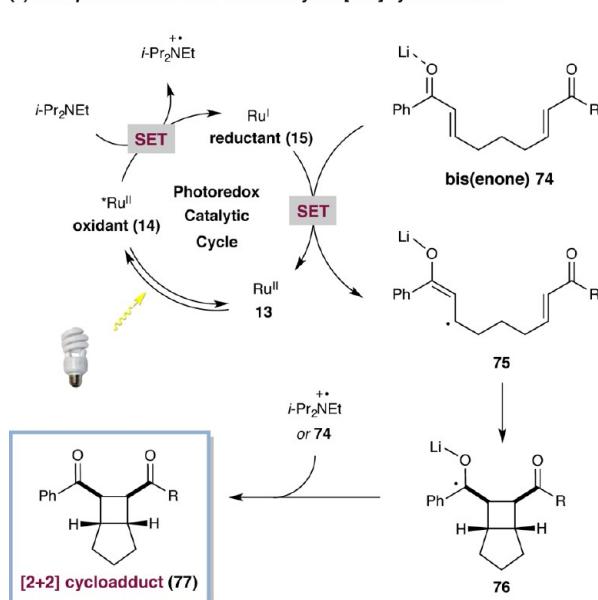
(b) *Yoon – Photoredox Lewis acid-catalyzed [3+2] cycloadditions*

cyclopropyl ketone

55–86% yield
16 examples
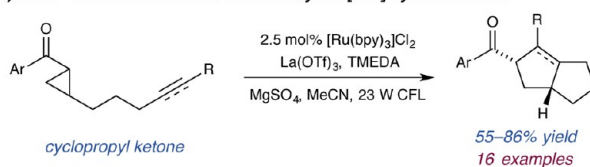
(c) *Xia – Photoredox Lewis acid-catalyzed reductive cyclization*

chalcone

40–84% yield
10 examples
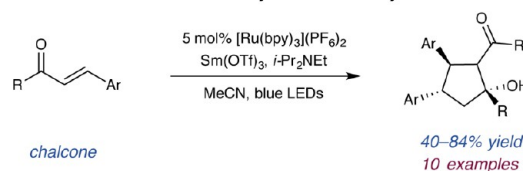
(d) *Yoon – Photoredox Lewis acid-catalyzed hetero-Diels Alder*

bis(enone)

5–86% yield
14 examples
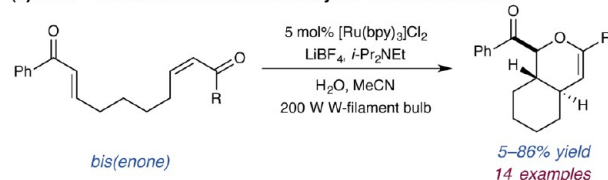
As discussed previously, Yoon demonstrated that bis-(enones) undergo intramolecular [2 + 2] cycloadditions when exposed to a dual photoredox Lewis acid catalyst system (see Scheme 2a).[14] In the proposed mechanism, there are three key reaction components required to mediate the formation of cycloadduct **77**; the photocatalyst (**13**), the Lewis acid catalyst, and a tertiary amine base (Scheme 29). The photoexcited Ru(II) catalyst (**14**) undergoes reductive quenching with the tertiary amine base, i-Pr2NEt, to deliver Ru(I) photocatalyst **15**. Coordination of the Lewis acid catalyst to bis(enone) **74** activates the substrate toward single-electron reduction by the highly reducing Ru(I) species (**15**), thereby regenerating the Ru(II) ground state (**13**). Cyclization of radical **75** delivers ketyl radical **76** and subsequent SET with either the tertiary amine radical cation or a different molecule of the bis(enone) starting material (**74**) then delivers the desired [2 + 2] cycloadduct (**77**).

The design principles used to develop the outlined [2 + 2] cycloaddition methodology have been applied to the development of a wide range of related Lewis acid-mediated protocols. In particular, Yoon has shown that modulation of the strength of the Lewis acid facilitates activation of different types of Lewis basic carbonyl substrates. Consequently, in addition to intermolecular [2 + 2] cycloadditions,[142] Yoon has demonstrated that [3 + 2] cycloadditions involving cyclopropyl ketones provides access to related 5,5-cycloadducts (Scheme 29b).[143] Here, a stronger Lewis acid was required to facilitate efficient generation of the ketyl radical and this intermediate could then undergo cyclopropane ring opening and cyclization onto a variety of alkene/alkyne acceptors. Xia and co-workers demonstrated that chalcones exhibit different reactivity in intermolecular dimerization reactions compared with the [2 + 2] cycloaddition pathway reported for alkyl-substituted enones (Scheme 29c). Under visible light irradiation, in the presence of a photoredox Lewis acid catalyst system, chalcones undergo reductive dimerization to deliver cyclopentanols. These products are proposed to form via radical anion dimerization, followed by protonation and aldol cyclization.[144] Yoon and co-workers also observed divergent reactivity when bis(enones) with an extended tether length were exposed to dual photoredox Lewis acid catalysis conditions (Scheme 29d).[145] In this case, radical anion hetero-Diels–Alder cycloaddition adducts were formed in lieu of the expected [2 + 2] cycloaddition adducts.

In addition to demonstrating that Lewis acid catalysts can modulate the reduction potential of enones to induce electron transfer, Yoon has also demonstrated that chiral Lewis acid complexes can impart stereocontrol in intermolecular [2 + 2] cycloadditions (Scheme 30).[146] Utilizing Eu(OTf)3 with dipeptide-derived chiral ligand **78** led to formation of the 1,2-*trans*-isomers of the [2 + 2] cycloadducts (**80**) with high levels of enantiocontrol. Interestingly, by simply switching to saturated dipeptide ligand **79**, the 1,2-*cis*-isomers of the products (**81**) were generated preferentially. In this protocol, the requirement of the Lewis acid for both reactivity and stereoselectivity prevents detrimental racemic background cycloadditions from occurring and, consequently, both isomeric products were generated in a highly enantioselective manner. More recently, Yoon has demonstrated that the previously discussed [3 + 2] cycloadditions involving cyclopropyl ketones (see Scheme 29b) can be rendered both intermolecular and asymmetric through the use of Gd(OTf)3 ligated with a chiral PyBox-derived ligand as the Lewis acid catalyst.[147]

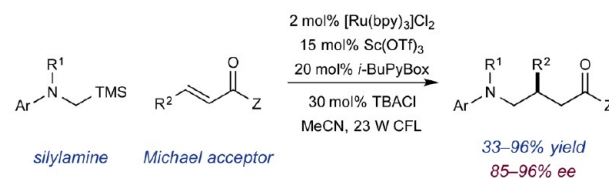**Scheme 30. Enantioselective Dual Photoredox Lewis Acid-Catalyzed Cycloadditions**

Yoon – Dual catalytic enantioselective [2+2] cycloadditions

ligand **78** - unsaturated imine
ligand **79** - saturated amine
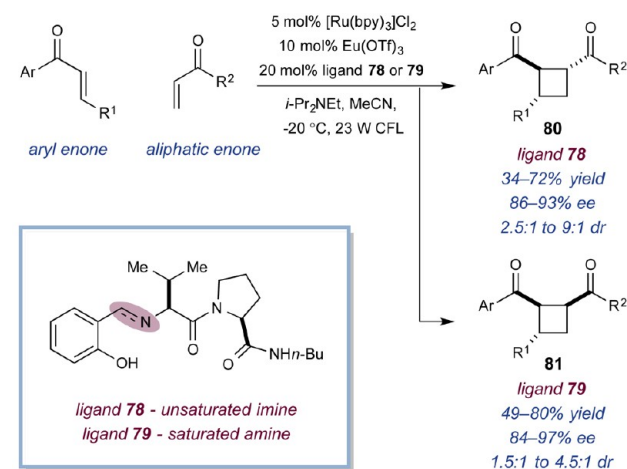
Dual photoredox Lewis acid-catalyzed reactions have also been developed in which the Lewis acid catalyst is not directly involved in the radical generation/stabilization events.[148] In this regard, catalytic protocols which utilize Lewis acids to enhance the rate of radical trapping have been reported.[149] Of particular note is a report by Yoon and co-workers demonstrating that conjugate additions of α-amino radicals can be rendered asymmetric through the use of a chiral i-BuPyBox-ligated Lewis acid catalyst (Scheme 31a).[33] Here, photoredox catalysis mediates generation of the α-amino radical and the Lewis acid complex controls stereoselectivity in the subsequent addition step. Recently, Meggers and co-workers reported a similar dual photoredox Lewis acid-catalyzed conjugate addition reaction that utilizes organotrifluoroborate salts as the source of

Scheme 31. Enantioselective Dual Photoredox Lewis Acid Catalysis

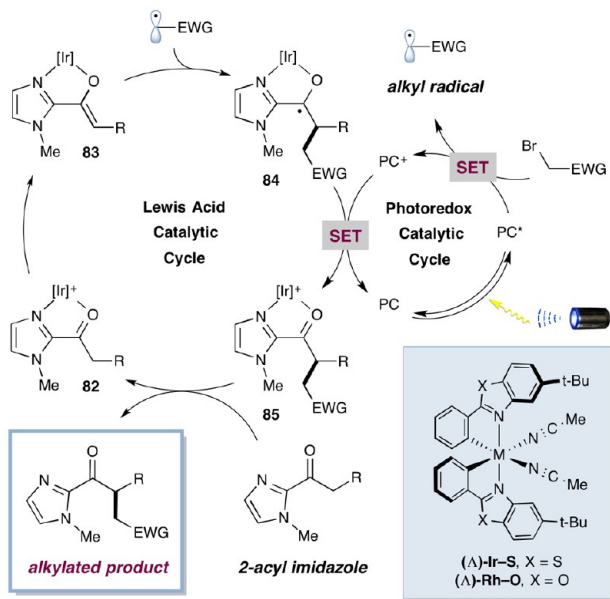(a) *Yoon – Enantioselective conjugate additions of α-amino radicals*

(b) *Meggers – Enantioselective dual catalytic radical conjugate additions*

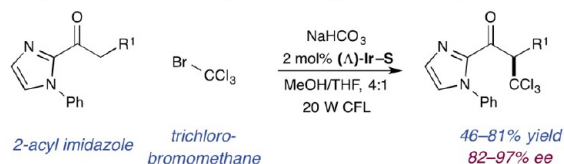*i*-BuPyBox   Z auxiliary   (Λ)-Rh–S
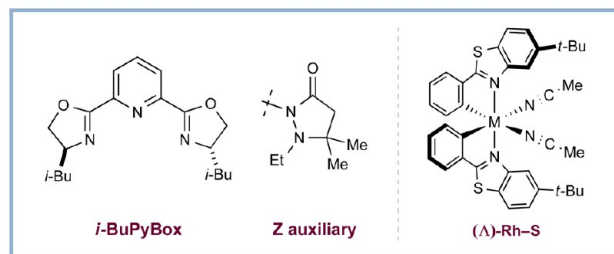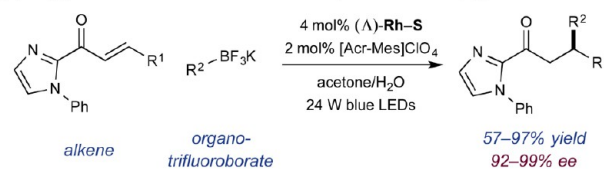
Scheme 32. Enantioselective Photoredox Protocols Mediated by Chiral Ir and Rh Catalysts

(a) *Meggers – Asymmetric photoredox catalysis using chiral Ir complexes*

(b) *Asymmetric trichloromethylations using a chiral Ir complex*

(c) *Asymmetric oxidative α-amino alkylations using a chiral Rh complex*

(d) *Asymmetric radical-radical couplings using a chiral Ir complex*

the alkyl radical coupling partner (Scheme 31b).[150] In this protocol, an organic dye was employed to mediate formation of the requisite alkyl radical and high levels of enantioselectivity were achieved using complex (Λ)-**Rh−S**, a Lewis acid catalyst that is chiral at the Rh center.

While the methodologies outlined in this section proceed through a number of mechanistically distinct pathways, a common feature for all these protocols is the use of a dual catalyst system composed of separate Lewis acid and photocatalyst components. Using a conceptually distinct approach, Meggers and co-workers have recently demonstrated that chiral Ir and Rh complexes, such as (Λ)-**Ir−S** and (Λ)-**Rh−O**, can function as both the Lewis acid catalyst and the photocatalyst precursor for a number of asymmetric transformations. In the initial report from Meggers, (Λ)-**Ir−S** was demonstrated as a competent catalyst for enantioselective alkylations of 2-acyl imidazole substrates (Scheme 32a).[151] The proposed mechanism involves initial complexation of the 2-acyl imidazole substrate to the (Λ)-**Ir−S** complex through displacement of the labile acetonitrile ligands, followed by deprotonation of **82** to Ir(III)−enolate complex **83**. In parallel, irradiation of a different molecule of the photoactive Ir complex, identified as complex **83** through mechanistic studies, delivers an excited Ir(III) photocatalyst which can reduce the alkyl bromide coupling partner to deliver an alkyl radical. Subsequent trapping of the alkyl radical by enolate **83** generates ketyl radical **84** which can then be oxidized by the Ir(IV) state of photocatalyst **83** to generate the catalyst-bound alkylated product (**85**). Complex **85** then undergoes ligand metathesis with another equivalent of substrate to regenerate complex **82** and deliver the desired product. In this reaction complex (Λ)-**Ir−S** functions as the Lewis acid catalyst, the precursor to photoactive Ir(III)−enolate complex **83** and is the source of chiral information in the enantiodetermining C−C bond-forming step. Using this design strategy, enantioselective trichloromethylations of 2-acyl imidazoles and pyridines have also been developed (Scheme 32b).[152]

In addition to redox-neutral C−H functionalizations, Meggers has demonstrated that enantioselective net oxidative

α-amino alkylations with α-silylamines[153] or tertiary amines[154] can be readily accomplished (Scheme 32c). In both of these protocols, oxygen is the terminal oxidant and in situ generation of an iminium ion is followed by trapping with the Lewis acid-bound enolate. Notably, the oxidative protocol outlined in Scheme 32c is catalyzed by a Rh(III) photoactive complex (derived from (Λ)-**Rh−O**), and this represents the first report of photomediated tertiary amine oxidation using a Rh(III) complex. Finally, Meggers has demonstrated that stereocontrolled radical−radical coupling reactions can be achieved using chiral (Λ)-**Ir−S** as both the Lewis acid catalyst and photoredox catalyst precursor (Scheme 32d).[155] This transformation represents a rare example of an enantioselective radical−radical coupling reaction (also see Scheme 11) and demonstrates the strength of utilizing a catalytic system wherein substrate reactivity is intrinsically linked with complexation to the asymmetric catalyst. Prior to these reports, the majority of visible light-mediated asymmetric protocols relied on using dual catalytic systems. The Meggers studies have elegantly demonstrated the opportunity for developing highly stereoselective monocatalytic photoredox protocols.

## ■ APPLICATIONS OF PHOTOREDOX CATALYSIS

Over the past eight years, the field of photoredox catalysis has experienced rapid growth, resulting in the development of a wide array of novel synthetic methodologies. Recent advances offer synthetic chemists novel bond disconnections and can provide protocols for the direct derivatization of native functional groups, such as C−H bonds and carboxylic acids. In addition, photoredox-catalyzed reactions generally proceed under extremely mild reaction conditions and this feature renders these technologies amenable to a large range of structurally and functionally diverse molecules. As such, it is not surprising that these methodologies have found utility in the synthesis of natural products and medicinally relevant compounds.[156] Initial reservations about the scalability of these protocols due to the inherent relationship between reaction efficiency and photon penetration have been addressed

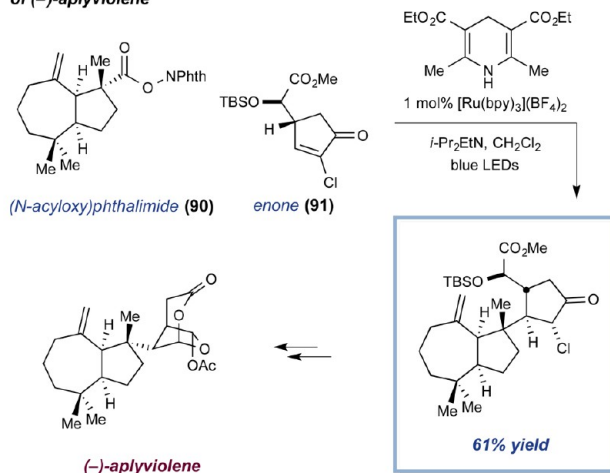## Scheme 33. Natural Product Syntheses Involving a Photoredox-Catalyzed Key Step

(a) *Yoon – Photoredox-catalyzed radical cation Diels-Alder for the synthesis of heitziamide A*
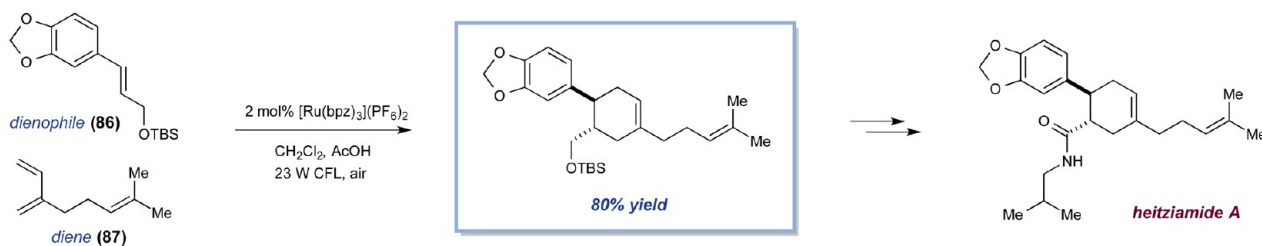
(b) *Stephenson – Photoredox-catalyzed reductive coupling for the synthesis of (+)-gliocladin C*
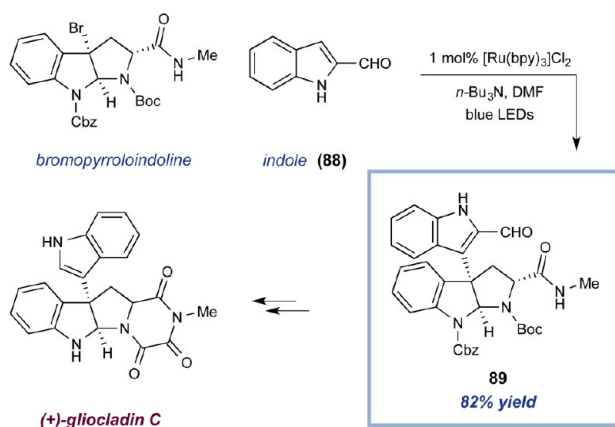
(c) *Overman – Photoredox-catalyzed radical conjugate addition for the synthesis of (−)-aplyviolene*

by the successful translation of batch photoredox-catalyzed reactions into large-scale flow protocols. Consequently, these technologies are now gaining considerable interest from industrial chemists both in the context of small-scale synthetic applications, such as late-stage functionalization in medicinal chemistry, and for large scale production of intermediates using flow. Herein, we will discuss key reports which highlight the utility of photoredox catalysis in the synthesis of complex molecular scaffolds and the application of this catalysis platform to medicinal chemistry.

Natural Product Synthesis. For many years, photochemical transformations have found widespread use in natural product synthesis due to the ability to access unusual modes of reactivity that are often thermally disallowed.[1] While the field of modern photoredox catalysis is comparatively new, this mode of photoactivation can offer some distinct advantages in the context of natural product synthesis. In particular, the use of visible light rather than UV light enables selective excitation of the photoredox catalyst in preference to most organic molecules. Consequently, the use of a low energy light source can prevent detrimental substrate/product degradation pathways from occurring in structurally complex molecules with sensitive functionality. Recently, a number of groups have demonstrated that photoredox catalysis can facilitate the construction of complex molecules by enabling previously challenging bond disconnections.

Yoon and co-workers have demonstrated that photoredox catalysis can facilitate thermally disfavored cycloaddition reactions through the generation of radical cation intermediates.[157,158] Using this strategy, electron-rich dienes and dienophiles underwent efficient [4 + 2] cycloadditions, wherein oxidation of the dienophile component to a radical cation

enabled these electronically mismatched Diels–Alder reactions to proceed. The outlined radical cation cycloaddition methodology was applied toward the synthesis of heitziamide A (Scheme 33a). Here, electron-rich dienophile **86** and diene **87** underwent efficient cyclization upon exposure to visible light and a photocatalyst. The corresponding cycloadduct could then be converted to the natural product in four steps. Notably, under thermal conditions, the diene/dienophile fragments corresponding to the natural product (not shown) underwent cyclization to deliver the unnatural regioisomer of heitziamide A. This result highlights the reversal in reactivity exhibited by the radical cation in comparison to the parent alkene. As previously mentioned, Nicewicz has also exploited photoredox-mediated alkene radical cation generation in the context of developing novel cycloaddition manifolds (see Scheme 14). The development of polar radical crossover cycloaddition reactions involving alkenes and unsaturated acids enabled the synthesis of a range of substituted γ-butyrolactones, and this methodology was successfully applied to the synthesis of racemic methylenolactocin and protolichesterinic acid.[66b]

In 2011, Stephenson demonstrated that (+)-gliocladin C could be synthesized by employing photoredox catalysis to facilitate the key indole-pyrroloindoline coupling step (Scheme 33b).[159] Seminal studies by the same laboratory had demonstrated that reductive dehalogenation of bromopyrroloindolines could be accomplished under mild conditions upon exposure to visible light and a photoredox catalyst (see Scheme 2c).[16] It was anticipated that the intermediate benzylic radical could be trapped with an indole. While unsubstituted indoles coupled to give the undesired C3−C2′ regioisomer, substituted indole **88** coupled efficiently to give the desired C3−C3′ regioisomer **89** in 82% yield. The realization of this coupling

strategy enabled the synthesis of (+)-gliocladin C, a key intermediate in the synthesis of other bisindole alkaloids, in 10 steps and 30% overall yield.

A second-generation synthesis of (−)-aplyviolene was reported by Overman in 2012, and in that publication, development of a photoredox-catalyzed conjugate addition reaction resulted in significant streamlining of the synthetic route (vs the first-generation approach).[108a,160] Reductive photoredox-mediated fragmentation of (N-acyloxy)phthalimide **90** generates a tertiary radical species which can intercept enone **91** to generate adjacent quaternary and tertiary stereocenters with high levels of diastereocontrol (Scheme 33c). Interestingly, Overman reported that an analogous conjugate addition with an organocuprate delivered exclusively a product that was epimeric at the quaternary stereocenter.[161] This elegant synthesis highlights the capacity of radical nucleophiles to exhibit distinct reactivity vs organometallic intermediates and generate challenging, sterically encumbered bonds.

Medicinal and Process Chemistry. While the scope of new synthetic methodologies is often examined using a range of relatively simple reaction partners, several academic groups have recently looked to apply their technologies toward the synthesis of more complex, druglike compounds to probe their generality. For example, Koike and Akita[162] along with our laboratory[38] demonstrated that photoredox-catalyzed conjugate additions of α-amino radicals could be applied toward the concise racemic syntheses of baclofen and pregabalin, respectively. In a collaboration with Eli Lilly, Stephenson demonstrated that photoredox-mediated coupling of N-methylmorpholine with pyridazine **92** provides rapid access to an intermediate in the synthesis of JAK2 inhibitor LY2784544 (Scheme 34a).[163] Here, a range of analogues could be readily synthesized by simply employing different tertiary amine coupling partners. In addition, recent advances from our group in the field of metallaphotoredox has enabled the rapid construction of medicinally relevant compounds such as fenofibrate[118] and edivoxetine·HCl[121] (Scheme 34b).

In a more general sense, the development of new methodologies that facilitate the construction of challenging C−C and C−heteroatom bonds in a robust and reliable manner over a broad range of substrates is highly desirable. Merck laboratories have developed a strategy for reliably evaluating and comparing transition metal-catalyzed cross-coupling methods by using chemistry informer libraries.[164] The libraries consist of a representative range of complex, pharmaceutically relevant coupling partners, such as boronic acids and aryl halides. Screening catalytic conditions against these libraries provides rapid insight into the scope and limitations of a methodology. In order to evaluate the generality of our recently reported photoredox Ni-catalyzed C−N cross-coupling protocol (see Scheme 26d), Merck laboratories submitted a chemistry informer library of druglike aryl halides to photoredox Ni amination conditions, with piperidine as the amine coupling partner.[131] This study revealed that 78% of the aryl halides underwent successful coupling. Given the importance of C−N cross-coupling to medicinal chemists, we were pleased to find that this result represents one of the highest success rates observed by Merck for a single aryl amination protocol and again serves to highlight the applicability of photoredox catalysis in an industrial setting.
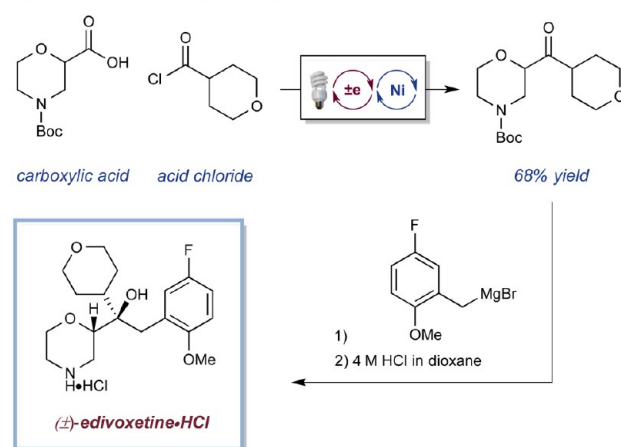
Late-stage functionalization is an important strategy within drug discovery and enables medicinal chemists access to

Scheme 34. Photoredox-Mediated Syntheses of Pharmaceutically Relevant Compounds

(a) *Stephenson – Photoredox-catalyzed α-amino C−H arylation*
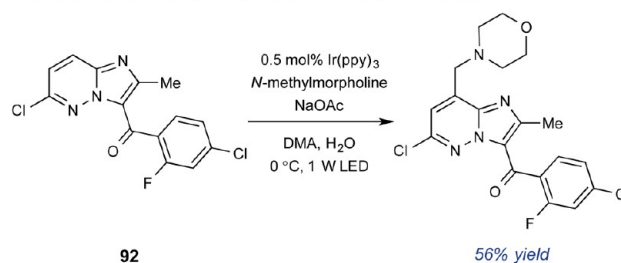
(b) *Photoredox Ni-catalyzed CO_2 extrusion–recombination*
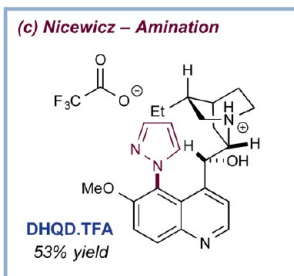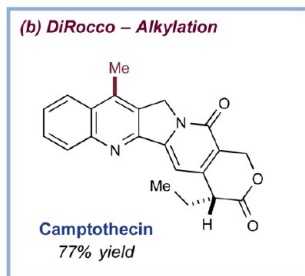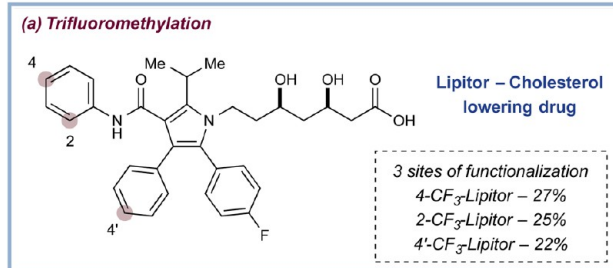
derivatives of drug candidates in a highly expeditious manner. The unique ability of photoredox catalysis to generate reactive radical intermediates under exceptionally mild conditions makes it suitable for late-stage functionalization of complex druglike molecules. In this regard, direct functionalization of C−H bonds represents an ideal solution as such bonds will be present in almost all drug candidates. In 2011, our group developed a method for direct C−H trifluoromethylation of arenes and heteroarenes.[165] Utilizing this methodology, a variety of biologically active compounds could be functionalized in high yields and the site selectivity of this protocol highlighted the metabolically susceptible positions on the arene substrate. Notably, Lipitor, one of the best-selling drugs of all time, underwent functionalization at three distinct positions (Scheme 35a).

In a subsequent report, DiRocco and co-workers, scientists at Merck Research Laboratories, demonstrated that direct C−H alkylation of heteroarenes could be achieved under photoredox catalysis conditions by utilizing peroxides as the source of alkyl radical (Scheme 35b).[166] Under the optimized conditions, methylation, ethylation and cyclopropanation of a range of medicinal and agrochemical agents could be achieved. By leveraging dual photoredox HAT catalysis, our group has demonstrated that simples alcohols can also be used as alkylating agents for heteroaromatic compounds and this protocol is driven by a key spin-center shift event (see Scheme 18).[77] This methodology was successfully applied to the alkylation of the medicinal agents fasudil and milrinone. More recently, Nicewicz demonstrated that direct C−H amination of druglike molecules could be achieved using his previously discussed dual photoredox HAT protocol (see Scheme 15).[69] This late-stage functionalization strategy differs from the

Scheme 35. Late-Stage Functionalization of Druglike Molecules via Photoredox-Catalyzed Methodologies

Photoredox-mediated late-stage functionalization protocols

(a) Trifluoromethylation

Lipitor – Cholesterol lowering drug

3 sites of functionalization
4-CF$_3$-Lipitor – 27%
2-CF$_3$-Lipitor – 25%
4'-CF$_3$-Lipitor – 22%

(b) DiRocco – Alkylation

Camptothecin
77% yield

(c) Nicewicz – Amination

DHQD.TFA
53% yield

Figure 4. Process-scale photoredox flow reactor at Merck. Photo courtesy of Merck and Co. Inc. Copyright 2016 American Chemical Society.[168]

previously discussed methods as, instead of direct radical addition onto the aromatic ring, generation of the arene radical cation enables addition of a closed-shell nucleophile (Scheme 35c). Together, these reports highlight the applicability of photoredox catalysis to late-stage functionalization and indicate that the outlined methods could be used as tools for alkylation, trifluoromethylation, and amination of druglike compounds.

One of the most attractive features of photoredox catalysis is the capacity to readily convert visible light into chemical energy. Recently, chemists have striven to optimize the efficiency of photoredox-mediated reactions by increasing photon penetration to the reaction medium. This factor becomes increasingly important when reactions are conducted on a large scale and the potential issues associated with large-scale batch chemistry can be circumvented through the translation of photoredox catalysis into flow. Many different types of photoredox-mediated reactions have been demonstrated in flow and, in general, considerably higher reaction efficiencies are observed vs a batch setup.[167] For medicinal chemists, small-scale batch reactions are often sufficient for obtaining compounds for testing in a drug discovery program. However, process chemists require reliable and robust methods for generating chemicals on a large scale and continuous flow technologies are ideally suited for this purpose (Figure 4). In this regard, there have been a number of recent reports demonstrating the translation of industrially relevant photoredox-mediated protocols from batch to large-scale flow setups.
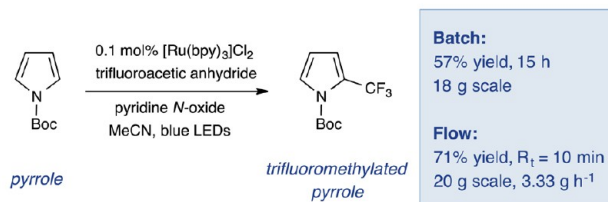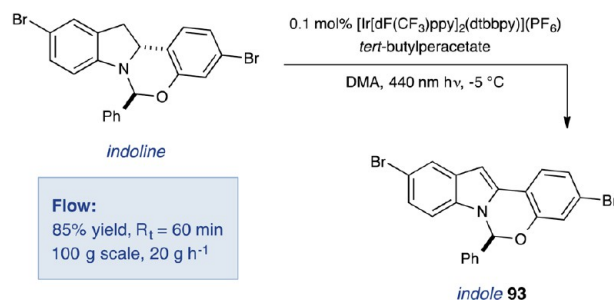
A new protocol for the C−H trifluoromethylation of arenes was developed through a collaboration between Stephenson and Eli Lilly.[169] Here, the key goals were to develop a scalable and inexpensive trifluoromethylation protocol that was operationally simple. Consequently, a method was developed which uses low-cost trifluoroacetic anhydride as the CF$_3$ source, with pyridine N-oxide as a sacrificial redox auxiliary. A wide variety of functionalized products could be generated and the reactions could be successfully scaled up to 5 g in a batch setup. Subsequently, Stephenson compared the reaction efficiency of the trifluoromethylation of N-Boc pyrrole in batch and flow and found the reaction was significantly more efficient in the latter,

generating 3.33 g of product per hour (vs 17.8 g over 15 h for batch) (Scheme 36a). The reaction was also scaled up to 100 g scale in batch and, although the reaction took 62 h, a 35% yield of the desired product was still obtained (vs 57% yield on 18 g scale). More recently, the Knowles group has collaborated with scientists at Merck to develop a photocatalytic dehydrogenation protocol for the synthesis of elbasvir, a NS5A antagonist for the treatment of hepatitis C.[170] Through these studies, a photoredox-mediated method was developed which enabled a high yield of indole **93** to be obtained with no erosion in the enantiopurity of the product (Scheme 36b). Mechanistic studies indicated that this reaction proceeds via a radical chain mechanism. Notably, the reaction could be scaled to 100 g using a flow system and high efficiency was observed (85% yield) with a throughput of 20 g/h. These reports demonstrate the applicability of continuous flow setups to large-scale photoredox reactions and highlight the potential for the use of photoredox-catalyzed methodologies on process scale.

Scheme 36. Application of Continuous Flow Setup to Photoredox-Catalyzed Methodologies

(a) Stephenson – Photoredox-catalyzed trifluoromethylation of arenes

0.1 mol% [Ru(bpy)$_3$]Cl$_2$
trifluoroacetic anhydride
pyridine N-oxide
MeCN, blue LEDs

pyrrole → trifluoromethylated pyrrole

Batch:
57% yield, 15 h
18 g scale

Flow:
71% yield, R$_t$ = 10 min
20 g scale, 3.33 g h^{-1}

(b) Knowles – Photocatalytic indoline dehydrogenation

0.1 mol% [Ir[dF(CF$_3$)ppy]$_2$(dtbbpy)](PF$_6$)
tert-butylperacetate
DMA, 440 nm hν, -5 °C

indoline →

Flow:
85% yield, R$_t$ = 60 min
100 g scale, 20 g h^{-1}

indole **93**

CONCLUSIONS AND OUTLOOK

Over the span of just eight years, the field of modern photoredox catalysis has experienced significant growth and a wide array of new activation platforms and synthetic transformations have been developed. Key to the development of these technologies is the ability of photoredox catalysts to efficiently convert visible light into chemical energy. In addition, through modification of the ligand backbone on metal polypyridyl photoredox catalysts, the redox properties of these complexes can be easily fine-tuned to suit almost any specific application. In a practical sense, the rapid uptake of photoredox catalysis by the chemical community stems from both the ease of reaction setup, using simple household light sources, and from the ability to access highly reactive radical intermediates from bench-stable precursors. Previous work focused on the generation and reactivity of C-centered radicals has been hindered by the toxicity of the tin reagents utilized as radical precursors. Recent advances in photoredox catalysis have demonstrated that a broad array of radical intermediates can be accessed from readily available chemicals such as carboxylic acids and halides and, in some cases, through direct homolysis of C−H bonds, thereby expanding the range of methods for native functionalization. In addition to providing new entries to the desired radical intermediates, photoredox catalysis has proven uniquely effective for the design of novel redox-neutral reaction manifolds. As a result of these characteristics, photoredox reactions have been developed which allow access to novel bond disconnections and facilitate the streamlining of synthetic strategies.

Despite these advances, we feel that the field of photoredox catalysis is still in its infancy with many exciting opportunities lying just around the corner. For example, the recent development of dual photoredox catalytic platforms has provided new activation modes that enable synthetic transformations to proceed in a highly regio- and enantioselective manner. These reports challenge the long-held belief that radical transformations are difficult to render enantioselective via asymmetric catalysis. In this regard, we anticipate that by leveraging dual catalytic strategies, such as the combination of photoredox with transition metal catalysis and hydrogen bonding catalysis, further development of highly enantioselective protocols will be possible. Moreover, dual photoredox organocatalysis has proven particularly effective for the development of methods for highly regioselective homolytic bond cleavage. Examples from the Knowles group and our own laboratory have demonstrated that hydrogen bonding catalysis can facilitate selective hydrogen atom transfer events. Of particular note is the development of multicatalytic strategies that enable direct, selective C−H functionalization, protocols that are attractive for the late-stage functionalization of druglike molecules. Studies in our laboratory have shown that the selectivity of organocatalytic HAT C−H functionalization protocols can be controlled by a combination of steric and electronic factors and, as a result, selective activation of hydridic C−H bonds can be achieved. Consequently, combined hydrogen bonding HAT catalysis platforms hold potential for targeting native functionality in a highly selective manner. One of the most recent modes of dual catalysis that has been developed is metallaphotoredox—the merger of photoredox catalysis and transition metal catalysis. This catalytic platform has gained significant attention from the synthetic community over the last four years due to the ability to modulate the oxidation state of the transition metal complex via photoredox-mediated radical generation or through direct SET events. As such, novel mechanistic pathways can be accessed that allow challenging C−C and C−X bonds to be formed.

To date, the ability of metal polypyridyl complexes and organic dye catalysts to facilitate triplet sensitization via an energy transfer process has not been extensively investigated. This mechanistic paradigm differs from photoredox catalysis in that molecules that cannot undergo redox chemistry with the excited state of the photocatalyst directly can instead be excited to their triplet state. This mechanistic manifold was utilized in the development of a copper photoredox-catalyzed C−N coupling protocol by the Kobayashi laboratory, and this report particularly highlights the potential of this strategy for the design of novel transition metal-catalyzed protocols.[171] The long-lived electronically excited states of the first-row transition metals can be difficult to access due to the quantum mechanically forbidden nature of intersystem crossing and the low degree of spin−orbit coupling. However, by utilization of a photocatalyst which readily accesses the triplet manifold and can subsequently transfer energy to a second metal catalyst, it should be feasible to "switch on" a range of mechanistic steps, which cannot be accessed in a traditional setting thereby enabling the development of novel reactions.

Considering these advances and the potential impact of further work in this field, the pharmaceutical industry has chosen to adopt these technologies at an unprecedented rate. Early work on their part has demonstrated that these catalytic platforms can be readily scaled up using flow technology. Given these successes we suspect that the surge of interest in photoredox catalysis will only lead to increased investigation and optimization of flow chemistry, as such we believe the future of these two fields remain intimately linked. In light of the advances in the field of photoredox catalysis we anticipate further adoption of this mode of catalysis in organic synthesis.

AUTHOR INFORMATION

Corresponding Author

*E-mail: dmacmill@princeton.edu.

Notes

The authors declare no competing financial interest.

Biographies

Megan H. Shaw obtained her MChem degree from the University of Sheffield in 2010. Following this, she conducted her Ph.D. studies under the supervison of Dr. John Bower at the University of Bristol, with co-supervision from Dr. William Whittingham at Syngenta. In 2015, she began a postdoctoral appointment with Professor David

MacMillan at Princeton University where she has focused on the development of C−H functionalization methodology through the merger of photoredox, HAT, and nickel catalysis.

Jack Twilton received his MChem degree from the University of Oxford in 2014, undertaking his final year project in the laboratory of Professor Veronique Gouverneur. He subsequently joined the group of Professor David MacMillan at Princeton University for his doctoral studies where he is currently working on the development of dual photoredox transition metal-catalyzed processes.

Dave MacMillan received his undergraduate degree in chemistry at the University of Glasgow, where he worked with Dr. Ernie Colvin. In 1990, he began his doctoral studies under the direction of Professor Larry Overman at the University of California, Irvine, before undertaking a postdoctoral position with Professor Dave Evans at Harvard University (1996). He began his independent career at the University of California, Berkeley, in July of 1998 before moving to Caltech in June of 2000 (Earle C. Anthony Chair of Organic Chemistry). In 2006, Dave moved to the east coast of the US to become the James S. McDonnell Distinguished University Professor at Princeton University, and he served as Department Chair from 2010 to 2015. Dave has received several awards, including the Janssen Pharmaceutica Prize (2016), Max Tischler Prize Harvard (2016), Ernst Schering Award in Biology, Chemistry and Medicine, Germany (2015), ACS Harrison Howe Award (2014), NJ ACS Molecular Design Award (2014), ACS Award for Creativity in Synthesis (2011), the Mitsui Catalysis Award (2011), ACS Cope Scholar Award (2007), ACS EJ Corey Award (2005), and the Corday−Morgan Medal (2005). Dave is a Fellow of the Royal Society (FRS) and the American Academy of Arts and Science. Dave helped launch and was Editor-in-Chief of *Chemical Sciences* (2009−1014) and is currently Chair of the NIH Study Section SBCA.

REFERENCES

(1) For reviews on the use of organic photochemistry in total synthesis, see: (a) Kärkäs, M. D.; Porco, J. A., Jr.; Stephenson, C. R. J. *Chem. Rev.* **2016**, DOI: 10.1021/acs.chemrev.5b00760. (b) Bach, T.; Hehn, J. P. *Angew. Chem., Int. Ed.* **2011**, *50*, 1000−1045. (c) Hoffmann, N. *Chem. Rev.* **2008**, *108*, 1052−1103. For a discussion on the early history of organic photochemistry, see: (d) Roth, H. D. *Angew. Chem., Int. Ed. Engl.* **1989**, *28*, 1193−1207. For early publications on organic photochemistry, see: (e) Trommsdorff, H. *Ann. Pharm.* **1834**, *11*, 190−207. (f) Ciamician, G.; Silber, P. *Ber. Dtsch. Chem. Ges.* **1908**, *41*, 1928−1935.

(2) (a) Grätzel, M. *Acc. Chem. Res.* **1981**, *14*, 376−384. (b) Meyer, T. J. *Acc. Chem. Res.* **1989**, *22*, 163−170.

(3) Takeda, H.; Ishitani, O. *Coord. Chem. Rev.* **2010**, *254*, 346−354.

(4) Kalyanasundaram, K.; Grätzel, M. *Coord. Chem. Rev.* **1998**, *177*, 347−414.

(5) For reviews on the field of photoredox catalysis, see: (a) Narayanam, J. M. R.; Stephenson, C. R. J. *Chem. Soc. Rev.* **2011**, *40*, 102−113. (b) Xuan, J.; Xiao, W.-J. *Angew. Chem., Int. Ed.* **2012**, *51*, 6828−6838. (c) Reckenthäler, M.; Griesbeck, A. G. *Adv. Synth. Catal.* **2013**, *355*, 2727−2744. (d) Prier, C. K.; Rankic, D. A.; MacMillan, D. W. C. *Chem. Rev.* **2013**, *113*, 5322−5363. (e) Schultz, D. M.; Yoon, T. P. *Science* **2014**, *343*, 1239176−1−1239176−8. (f) Skubi, K. L.; Blum, T. R.; Yoon, T. P. *Chem. Rev.* **2016**, DOI: 10.1021/acs.chemrev.6b00018. (g) Romero, N. A.; Nicewicz, D. A. *Chem. Rev.* **2016**, DOI: 10.1021/acs.chemrev.6b00057.

(6) The triplet energy of $Ir(ppy)_3$ $[Ir(ppy)_3 = Ir(2\text{-phenylpyridinato-}C2,N)_3]$ can be estimated as 56.5 kcal mol^{-1} given that the phosphorescence emission corresponding to the T1 to S0 0−0 transition occurs at 19712 cm^{-1}. Hofbeck, T.; Yersin, H. *Inorg. Chem.* **2010**, *49*, 9290−9299.

(7) (a) Hedstrand, D. M.; Kruizinga, W. M.; Kellogg, R. M. *Tetrahedron Lett.* **1978**, *19*, 1255−1258. (b) van Bergen, T. J.; Hedstrand, D. M.; Kruizinga, W. H.; Kellogg, R. M. *J. Org. Chem.* **1979**, *44*, 4953−4962.

(8) (a) Hironaka, K.; Fukuzumi, S.; Tanaka, T. *J. Chem. Soc., Perkin Trans. 2* **1984**, 1705−1709. (b) Fukuzumi, S.; Koumitsu, S.; Hironaka, K.; Tanaka, T. *J. Am. Chem. Soc.* **1987**, *109*, 305−316. (c) Fukuzumi, S.; Mochizuki, S.; Tanaka, T. *J. Phys. Chem.* **1990**, *94*, 722−726.

(9) (a) Pac, C.; Ihama, M.; Yasuda, M.; Miyauchi, Y.; Sakurai, H. *J. Am. Chem. Soc.* **1981**, *103*, 6495−6497. (b) Pac, C.; Miyauchi, Y.; Ishitani, O.; Ihama, M.; Yasuda, M.; Sakurai, H. *J. Org. Chem.* **1984**, *49*, 26−34. (c) Ishitani, O.; Ihama, M.; Miyauchi, Y.; Pac, C. *J. Chem. Soc., Perkin Trans. 1* **1985**, 1527−1531. (d) Ishitani, O.; Pac, C.; Sakurai, H. *J. Org. Chem.* **1983**, *48*, 2941−2942. (e) Ishitani, O.; Yanagida, S.; Takamuku, S.; Pac, C. *J. Org. Chem.* **1987**, *52*, 2790−2796.

(10) Cano-Yelo, H.; Deronzier, A. *Tetrahedron Lett.* **1984**, *25*, 5517−5520.

(11) (a) Cano-Yelo, H.; Deronzier, A. *J. Chem. Soc., Perkin Trans. 2* **1984**, 1093−1098. (b) Cano-Yelo, H.; Deronzier, A. *J. Photochem.* **1987**, *37*, 315−321.

(12) Okada, K.; Okamoto, K.; Morita, N.; Okubo, K.; Oda, M. *J. Am. Chem. Soc.* **1991**, *113*, 9401−9402.

(13) For protocols utilizing UV light, see: (a) Okada, K.; Okamoto, K.; Oda, M. *J. Am. Chem. Soc.* **1988**, *110*, 8736−8738. (b) Okada, K.; Okamoto, K.; Oda, M. *J. Chem. Soc., Chem. Commun.* **1989**, 1636−1637. For protocols utilizing visible light, see: (c) Okada, K.; Okubo, K.; Morita, N.; Oda, M. *Tetrahedron Lett.* **1992**, *33*, 7377−7380. (d) Okada, K.; Okubo, K.; Morita, N.; Oda, M. *Chem. Lett.* **1993**, *22*, 2021−2024.

(14) Ischay, M. A.; Anzovino, M. E.; Du, J.; Yoon, T. P. *J. Am. Chem. Soc.* **2008**, *130*, 12886−12887.

(15) Nicewicz, D. A.; MacMillan, D. W. C. *Science* **2008**, *322*, 77−80.

(16) Narayanam, J. M. R.; Tucker, J. W.; Stephenson, C. R. J. *J. Am. Chem. Soc.* **2009**, *131*, 8756−8757.

(17) Data were obtained by a search of the Thomson Reuters Web of Science for the keyword photoredox catalysis and its derivatives. The results were evaluated and refined to remove articles that were not directly relevant to photoredox catalysis in the context of organic synthesis. This search is unlikely to have found all publications on photoredox catalysis, and a conservative estimate is that more than 700 manuscripts have been published on this topic so far.

(18) Vitaku, E.; Smith, D. T.; Njardarson, J. T. *J. Med. Chem.* **2014**, *57*, 10257−10274.

(19) (a) Condie, A. G.; González-Gómez, J. C.; Stephenson, C. R. J. *J. Am. Chem. Soc.* **2010**, *132*, 1464−1465. (b) Freeman, D. B.; Furst, L.; Condie, A. G.; Stephenson, C. R. J. *Org. Lett.* **2012**, *14*, 94−97. For subsequent work using rose bengal as the photocatalyst, see: (c) Pan, Y.; Kee, C. W.; Chen, L.; Tan, C.-H. *Green Chem.* **2011**, *13*, 2682−2685.

(20) Estimation of the pK_a of the α-C−H bond of amine radical cations can be performed according to eq 19 found in: Nicholas, A. M. de P.; Arnold, D. R. *Can. J. Chem.* **1982**, *60*, 2165−2179.

(21) Liu, Q.; Li, Y.-N.; Zhang, H.-H.; Chen, B.; Tung, C.-H.; Wu, L.-Z. *Chem. - Eur. J.* **2012**, *18*, 620−627.

(22) Pan, Y.; Wang, S.; Kee, C. W.; Dubuisson, E.; Yang, Y.; Loh, K. P.; Tan, C.-H. *Green Chem.* **2011**, *13*, 3341−3344.

(23) (a) Dai, C.; Meschini, F.; Narayanam, J. M. R.; Stephenson, C. R. J. *J. Org. Chem.* **2012**, *77*, 4425−4431. The mechanism for this transformation proceeds via initial hydrogen atom abstraction (not amine oxidation). For an example where the mechanism proceeds via initial amine oxidation, see: (b) Wang, Z.-Q.; Hu, M.; Huang, X.-C.; Gong, L.-B.; Xie, Y.-X.; Li, J.-H. *J. Org. Chem.* **2012**, *77*, 8705−8711.

(24) Rueping, M.; Zhu, S.; Koenigs, R. M. *Chem. Commun.* **2011**, *47*, 8679−8681.

(25) (a) Xuan, J.; Feng, Z.-J.; Duan, S.-W.; Xiao, W.-J. *RSC Adv.* **2012**, *2*, 4065−4068. (b) Mathis, C. L.; Gist, B. M.; Frederickson, C. K.; Midkiff, K. M.; Marvin, C. C. *Tetrahedron Lett.* **2013**, *54*, 2101−2104.

(26) Rueping, M.; Vila, C.; Koenigs, R. M.; Poscharny, K.; Fabry, D. C. *Chem. Commun.* **2011**, *47*, 2360−2362.

(27) DiRocco, D. A.; Rovis, T. *J. Am. Chem. Soc.* **2012**, *134*, 8094−8097.

(28) Bergonzini, G.; Schindler, C. S.; Wallentin, C.-J.; Jacobsen, E. N.; Stephenson, C. R. J. *Chem. Sci.* **2014**, *5*, 112−116.

(29) Rueping, M.; Koenigs, R. M.; Poscharny, K.; Fabry, D. C.; Leonori, D.; Vila, C. *Chem. - Eur. J.* **2012**, *18*, 5170−5174.

(30) McNally, A.; Prier, C. K.; MacMillan, D. W. C. *Science* **2011**, *334*, 1114−1117.

(31) Miyake, Y.; Nakajima, K.; Nishibayashi, Y. *Chem. - Eur. J.* **2012**, *18*, 16473−16477.

(32) (a) Kohls, P.; Jadhav, D.; Pandey, G.; Reiser, O. *Org. Lett.* **2012**, *14*, 672−675. (b) Ruiz Espelt, L.; Wiensch, E. M.; Yoon, T. P. *J. Org. Chem.* **2013**, *78*, 4107−4114. (c) Zhu, S.; Das, A.; Bui, L.; Zhou, H.; Curran, D. P.; Rueping, M. *J. Am. Chem. Soc.* **2013**, *135*, 1823−1829. (d) Miyake, Y.; Nakajima, K.; Nishibayashi, Y. *J. Am. Chem. Soc.* **2012**, *134*, 3338−3341.

(33) Ruiz Espelt, L.; McPherson, I. S.; Wiensch, E. M.; Yoon, T. P. *J. Am. Chem. Soc.* **2015**, *137*, 2452−2455.

(34) Murphy, J. J.; Bastida, D.; Paria, S.; Fagnoni, M.; Melchiorre, P. *Nature* **2016**, *532*, 218−222.

(35) (a) Leung, J. C. T.; Chatalova-Sazepin, C.; West, J. G.; Rueda-Becerril, M.; Paquin, J.-F.; Sammis, G. M. *Angew. Chem., Int. Ed.* **2012**, *51*, 10804−10807. (b) Rueda-Becerril, M.; Mahé, O.; Drouin, M.; Majewski, M. B.; West, J. G.; Wolf, M. O.; Sammis, G. M.; Paquin, J.-F. *J. Am. Chem. Soc.* **2014**, *136*, 2637−2641. (c) Ventre, S.; Petronijevic, F. R.; MacMillan, D. W. C. *J. Am. Chem. Soc.* **2015**, *137*, 5654−5657. (d) Wu, X.; Meng, C.; Yuan, X.; Jia, X.; Qian, X.; Ye, J. *Chem. Commun.* **2015**, *51*, 11864−11867.

(36) Noble, A.; MacMillan, D. W. C. *J. Am. Chem. Soc.* **2014**, *136*, 11602−11605.

(37) Le Vaillant, F.; Courant, T.; Waser, J. *Angew. Chem., Int. Ed.* **2015**, *54*, 11200−11204.

(38) Chu, L.; Ohta, C.; Zuo, Z.; MacMillan, D. W. C. *J. Am. Chem. Soc.* **2014**, *136*, 10886−10889.

(39) (a) Cassani, C.; Bergonzini, G.; Wallentin, C.-J. *Org. Lett.* **2014**, *16*, 4228−4231. (b) Griffin, J. D.; Zeller, M. A.; Nicewicz, D. A. *J. Am. Chem. Soc.* **2015**, *137*, 11340−11348.

(40) Zuo, Z.; MacMillan, D. W. C. *J. Am. Chem. Soc.* **2014**, *136*, 5257−5260.

(41) (a) Beatty, J. W.; Stephenson, C. R. J. *Acc. Chem. Res.* **2015**, *48*, 1474−1484. (b) Shi, L.; Xia, W. *Chem. Soc. Rev.* **2012**, *41*, 7687−7697. (c) Hu, J.; Wang, J.; Nguyen, T. H.; Zheng, N. *Beilstein J. Org. Chem.* **2013**, *9*, 1977−2001.

(42) Nagib, D. A.; Scott, M. E.; MacMillan, D. W. C. *J. Am. Chem. Soc.* **2009**, *131*, 10875−10877.

(43) Shih, H.-W.; Vander Wal, M. N.; Grange, R. L.; MacMillan, D. W. C. *J. Am. Chem. Soc.* **2010**, *132*, 13600−13603.

(44) Welin, E. R.; Warkentin, A. A.; Conrad, J. C.; MacMillan, D. W. C. *Angew. Chem., Int. Ed.* **2015**, *54*, 9668−9672.

(45) Cecere, G.; König, C. M.; Alleva, J. L.; MacMillan, D. W. C. *J. Am. Chem. Soc.* **2013**, *135*, 11521−11524.

(46) Zhu, Y.; Zhang, L.; Luo, S. *J. Am. Chem. Soc.* **2014**, *136*, 14642−14645.

(47) (a) Gualandi, A.; Marchini, M.; Mengozzi, L.; Natali, M.; Lucarini, M.; Ceroni, P.; Cozzi, P. G. *ACS Catal.* **2015**, *5*, 5927−5931. (b) Neumann, M.; Füldner, S.; König, B.; Zeitler, K. *Angew. Chem., Int. Ed.* **2011**, *50*, 951−954. (c) Neumann, M.; Zeitler, K. *Org. Lett.* **2012**, *14*, 2658−2661. (d) Fidaly, K.; Ceballos, C.; Falguières, A.; Sylla-Iyarreta Veitia, M.; Guy, A.; Ferroud, C. *Green Chem.* **2012**, *14*, 1293−1297.

(48) Jakobsen, H. J.; Lawesson, S.-O.; Marshall, J. T. B.; Schroll, G.; Williams, D. H. *J. Chem. Soc. B* **1966**, 940−946.

(49) Beeson, T. D.; Mastracchio, A.; Hong, J.-B.; Ashton, K.; MacMillan, D. W. C. *Science* **2007**, *316*, 582−585.

(50) Koike, T.; Akita, M. *Chem. Lett.* **2009**, *38*, 166−167.

(51) Pirnot, M. T.; Rankic, D. A.; Martin, D. B. C.; MacMillan, D. W. C. *Science* **2013**, *339*, 1593−1596.

(52) (a) Porter, N. A.; Giese, B.; Curran, D. P. *Acc. Chem. Res.* **1991**, *24*, 296−304. (b) Fischer, H.; Radom, L. *Angew. Chem., Int. Ed.* **2001**, *40*, 1340−1371.

(53) Petronijević, F. R.; Nappi, M.; MacMillan, D. W. C. *J. Am. Chem. Soc.* **2013**, *135*, 18323−18326.

(54) Jeffrey, J. L.; Petronijević, F. R.; MacMillan, D. W. C. *J. Am. Chem. Soc.* **2015**, *137*, 8404−8407.

(55) Terrett, J. A.; Clift, M. D.; MacMillan, D. W. C. *J. Am. Chem. Soc.* **2014**, *136*, 6858−6861.

(56) (a) Uraguchi, D.; Kinoshita, N.; Kizu, T.; Ooi, T. *J. Am. Chem. Soc.* **2015**, *137*, 13768−13771. (b) Kizu, T.; Uraguchi, D.; Ooi, T. *J. Org. Chem.* **2016**, DOI: 10.1021/acs.joc.6b00445.

(57) (a) Miller, D. C.; Tarantino, K. T.; Knowles, R. R. Proton-Coupled Electron Transfer in Organic Synthesis: Fundamentals, Applications and Opportunities. In *Topics in Current Chemistry*; Guillena, G., Ramón, D. J., Eds.; Springer International Publishing, 2016; Vol. 374, DOI: 10.1007/s41061-016-0030-6. (b) Yayla, H. G.; Knowles, R. R. *Synlett* **2014**, *25*, 2819−2826.

(58) Tarantino, K. T.; Liu, P.; Knowles, R. R. *J. Am. Chem. Soc.* **2013**, *135*, 10022−10025.

(59) Rono, L. J.; Yayla, H. G.; Wang, D. Y.; Armstrong, M. F.; Knowles, R. R. *J. Am. Chem. Soc.* **2013**, *135*, 17735−17738.

(60) Choi, G. J.; Knowles, R. R. *J. Am. Chem. Soc.* **2015**, *137*, 9226−9229.

(61) Miller, D. C.; Choi, G. J.; Orbe, H. S.; Knowles, R. R. *J. Am. Chem. Soc.* **2015**, *137*, 13492−13495.

(62) (a) Nechab, M.; Mondal, S.; Bertrand, M. P. *Chem. - Eur. J.* **2014**, *20*, 16034−16059. (b) Protti, S.; Fagnoni, M.; Ravelli, D. *ChemCatChem* **2015**, *7*, 1516−1523.

(63) Hamilton, D. S.; Nicewicz, D. A. *J. Am. Chem. Soc.* **2012**, *134*, 18577−18580.

(64) Perkowski, A. J.; Nicewicz, D. A. *J. Am. Chem. Soc.* **2013**, *135*, 10334−10337.

(65) (a) Nguyen, T. M.; Nicewicz, D. A. *J. Am. Chem. Soc.* **2013**, *135*, 9588−9591. (b) Nguyen, T. M.; Manohar, N.; Nicewicz, D. A. *Angew. Chem., Int. Ed.* **2014**, *53*, 6198−6201.

(66) (a) Grandjean, J.-M. M.; Nicewicz, D. A. *Angew. Chem., Int. Ed.* **2013**, *52*, 3967−3971. (b) Zeller, M. A.; Riener, M.; Nicewicz, D. A. *Org. Lett.* **2014**, *16*, 4810−4813. (c) Gesmundo, N. J.; Grandjean, J.-M. M.; Nicewicz, D. A. *Org. Lett.* **2015**, *17*, 1316−1319. (d) Cavanaugh, C. L.; Nicewicz, D. A. *Org. Lett.* **2015**, *17*, 6082−6085.

(67) Wilger, D. J.; Grandjean, J.-M. M.; Lammert, T. R.; Nicewicz, D. A. *Nat. Chem.* **2014**, *6*, 720−726.

(68) (a) Ohkubo, K.; Kobayashi, T.; Fukuzumi, S. *Angew. Chem., Int. Ed.* **2011**, *50*, 8652−8655. (b) Ohkubo, K.; Fujimoto, A.; Fukuzumi, S. *J. Phys. Chem. A* **2013**, *117*, 10719−10725.

(69) Romero, N. A.; Margrey, K. A.; Tay, N. E.; Nicewicz, D. A. *Science* **2015**, *349*, 1326−1330.

(70) Schroll, P.; Hari, D. P.; König, B. *ChemistryOpen* **2012**, *1*, 130−133. (b) Hering, T.; Hari, D. P.; König, B. *J. Org. Chem.* **2012**, *77*, 10347−10352. (c) Yasu, Y.; Koike, T.; Akita, M. *Angew. Chem., Int. Ed.* **2012**, *51*, 9567−9571. (d) Pham, P. V.; Nagib, D. A.; MacMillan, D. W. C. *Angew. Chem., Int. Ed.* **2011**, *50*, 6119−6122. (e) Arai, Y.; Tomita, R.; Ando, G.; Koike, T.; Akita, M. *Chem. - Eur. J.* **2016**, *22*, 1262−1265.

(71) Mizuta, S.; Verhoog, S.; Engle, K. M.; Khotavivattana, T.; O'Duill, M.; Wheelhouse, K.; Rassias, G.; Médebielle, M.; Gouverneur, V. *J. Am. Chem. Soc.* **2013**, *135*, 2505−2508.

(72) Wilger, D. J.; Gesmundo, N. J.; Nicewicz, D. A. *Chem. Sci.* **2013**, *4*, 3160−3165.

(73) Cai, Y.; Roberts, B. P. *Chem. Commun.* **1998**, 1145−1146.

(74) Qvortrup, K.; Rankic, D. A.; MacMillan, D. W. C. *J. Am. Chem. Soc.* **2014**, *136*, 626−629.

(75) Hager, D.; MacMillan, D. W. C. *J. Am. Chem. Soc.* **2014**, *136*, 16986−16989.

(76) Cuthbertson, J. D.; MacMillan, D. W. C. *Nature* **2015**, *519*, 74−77.

(77) Jin, J.; MacMillan, D. W. C. *Nature* **2015**, *525*, 87−90.

(78) (a) Minisci, F.; Bernardi, R.; Bertini, F.; Galli, R.; Perchinummo, M. *Tetrahedron* **1971**, *27*, 3575−3579. (b) Duncton, M. A. J. *MedChemComm* **2011**, *2*, 1135−1161.

(79) Eklund, H.; Uhlin, U.; Färnegårdh, M.; Logan, D. T.; Nordlund, P. *Prog. Biophys. Mol. Biol.* **2001**, *77*, 177−268.

(80) H−N⁺ BDE [quinuclidine] = 100 kcal mol⁻¹: Liu, W.-Z.; Bordwell, F. G. *J. Org. Chem.* **1996**, *61*, 4778−4783. S−H BDE [methyl thioglycolate] = 87 kcal mol⁻¹: Escoubet, S.; Gastaldi, S.; Vanthuyne, N.; Gil, G.; Siri, D.; Bertrand, M. P. *J. Org. Chem.* **2006**, *71*, 7288−7292.

(81) Jeffrey, J. L.; Terrett, J. A.; MacMillan, D. W. C. *Science* **2015**, *349*, 1532−1536.

(82) Cradlebaugh, J. A.; Zhang, L.; Shelton, G. R.; Litwinienko, G.; Smart, B. E.; Ingold, K. U.; Dolbier, W. R., Jr. *Org. Biomol. Chem.* **2004**, *2*, 2083−2086.

(83) (a) Johansson Seechurn, C. C. C.; Kitching, M. O.; Colacot, T. J.; Snieckus, V. *Angew. Chem., Int. Ed.* **2012**, *51*, 5062−5085. (b) Nicolaou, K. C.; Bulger, P. G.; Sarlah, D. *Angew. Chem., Int. Ed.* **2005**, *44*, 4442−4489.

(84) Kalyani, D.; McMurtrey, K. B.; Neufeldt, S. R.; Sanford, M. S. *J. Am. Chem. Soc.* **2011**, *133*, 18566−18569.

(85) For transition metal-catalyzed reactions involving radicals generally proceed via single-electron oxidation state changes, see: (a) Jahn, U. *Top. Curr. Chem.* **2011**, *320*, 121−189. (b) Jahn, U. *Top. Curr. Chem.* **2011**, *320*, 191−322. (c) Jahn, U. *Top. Curr. Chem.* **2011**, *320*, 323−451.

(86) Osawa, M.; Nagai, H.; Akita, M. *Dalton Trans.* **2007**, 827−829.

(87) Diaryliodonium salts have since been shown as competent sources of aryl radical; see: Neufeldt, S. R.; Sanford, M. S. *Adv. Synth. Catal.* **2012**, *354*, 3517−3522.

(88) In a subsequent computational study, an alternative mechanistic pathway was proposed involving reductive elimination from Pd(III)

species **50** followed by SET to regenerate the active Pd(II) catalyst; see: Maestri, G.; Malacria, M.; Derat, E. *Chem. Commun.* **2013**, *49*, 10424−10426.

(89) Kalyani, D.; Deprez, N. R.; Desai, L. V.; Sanford, M. S. *J. Am. Chem. Soc.* **2005**, *127*, 7330−7331. For a review on transition metal-catalyzed C−H bond activation, see: Wencel-Delord, J.; Dröge, T.; Liu, F.; Glorius, F. *Chem. Soc. Rev.* **2011**, *40*, 4740−4761.

(90) Zoller, J.; Fabry, D. C.; Ronge, M. A.; Rueping, M. *Angew. Chem., Int. Ed.* **2014**, *53*, 13264−13268.

(91) Fabry, D. C.; Ronge, M. A.; Zoller, J.; Rueping, M. *Angew. Chem., Int. Ed.* **2015**, *54*, 2801−2805.

(92) Fabry, D. C.; Zoller, J.; Raja, S.; Rueping, M. *Angew. Chem., Int. Ed.* **2014**, *53*, 10228−10231.

(93) (a) Sahoo, B.; Hopkinson, M. N.; Glorius, F. *J. Am. Chem. Soc.* **2013**, *135*, 5505−5508. (b) Hopkinson, M. N.; Sahoo, B.; Glorius, F. *Adv. Synth. Catal.* **2014**, *356*, 2794−2800.

(94) Shu, X.-z.; Zhang, M.; He, Y.; Frei, H.; Toste, F. D. *J. Am. Chem. Soc.* **2014**, *136*, 5844−5847.

(95) Zhang, Q.; Zhang, Z.-Q.; Fu, Y.; Yu, H.-Z. *ACS Catal.* **2016**, *6*, 798−808.

(96) (a) Um, J.; Yun, H.; Shin, S. *Org. Lett.* **2016**, *18*, 484−487. (b) Tlahuext-Aca, A.; Hopkinson, M. N.; Garza-Sanchez, R. A.; Glorius, F. *Chem. - Eur. J.* **2016**, *22*, 5909−5913.

(97) (a) Kim, S.; Rojas-Martin, J.; Toste, F. D. *Chem. Sci.* **2016**, *7*, 85−88. (b) Tlahuext-Aca, A.; Hopkinson, M. N.; Sahoo, B.; Glorius, F. *Chem. Sci.* **2016**, *7*, 89−93.

(98) He, Y.; Wu, H.; Toste, F. D. *Chem. Sci.* **2015**, *6*, 1194−1198.

(99) For reviews on homogeneous gold catalysis, see: (a) Krause, N.; Winter, C. *Chem. Rev.* **2011**, *111*, 1994−2009. (b) Rudolph, M.; Hashmi, A. S. K. *Chem. Soc. Rev.* **2012**, *41*, 2448−2462. (c) Dorel, R.; Echavarren, A. M. *Chem. Rev.* **2015**, *115*, 9028−9072.

(100) Ye, Y.; Sanford, M. S. *J. Am. Chem. Soc.* **2012**, *134*, 9034−9037.

(101) Wang, J.; Sánchez-Roselló, M.; Aceña, J. L.; del Pozo, C.; Sorochinsky, A. E.; Fustero, S.; Soloshonok, V. A.; Liu, H. *Chem. Rev.* **2014**, *114*, 2432−2506.

(102) (a) Zultanski, S. L.; Fu, G. C. *J. Am. Chem. Soc.* **2011**, *133*, 15362−15364. (b) Dudnik, A. S.; Fu, G. C. *J. Am. Chem. Soc.* **2012**, *134*, 10693−10697. (c) Zultanski, S. L.; Fu, G. C. *J. Am. Chem. Soc.* **2013**, *135*, 624−627. (d) Schley, N. D.; Fu, G. C. *J. Am. Chem. Soc.* **2014**, *136*, 16588−16593.

(103) Zuo, Z.; Ahneman, D. T.; Chu, L.; Terrett, J. A.; Doyle, A. G.; MacMillan, D. W. C. *Science* **2014**, *345*, 437−440.

(104) Tellis, J. C.; Primer, D. N.; Molander, G. A. *Science* **2014**, *345*, 433−436.

(105) Computational studies have suggested that radical addition to nickel may occur prior to oxidative addition, and the sequence of these steps has not been fully determined; see: Gutierrez, O.; Tellis, J. C.; Primer, D. N.; Molander, G. A.; Kozlowski, M. C. *J. Am. Chem. Soc.* **2015**, *137*, 4896−4899.

(106) (a) Everson, D. A.; Shrestha, R.; Weix, D. J. *J. Am. Chem. Soc.* **2010**, *132*, 920−921. (b) Everson, D. A.; Jones, B. A.; Weix, D. J. *J. Am. Chem. Soc.* **2012**, *134*, 6146−6159. (c) Biswas, S.; Weix, D. J. *J. Am. Chem. Soc.* **2013**, *135*, 16192−16197. (d) Weix, D. J. *Acc. Chem. Res.* **2015**, *48*, 1767−1775.

(107) For a review on decarboxylative cross-coupling reactions, see: Rodríguez, N.; Gooßen, L. J. *Chem. Soc. Rev.* **2011**, *40*, 5030−5048.

(108) (a) Schnermann, M. J.; Overman, L. E. *Angew. Chem., Int. Ed.* **2012**, *51*, 9576−9580. (b) Pratsch, G.; Lackner, G. L.; Overman, L. E. *J. Org. Chem.* **2015**, *80*, 6025−6036.

(109) (a) Cornella, J.; Edwards, J. T.; Qin, T.; Kawamura, S.; Wang, J.; Pan, C.-M.; Gianatassio, R.; Schmidt, M.; Eastgate, M. D.; Baran, P. S. *J. Am. Chem. Soc.* **2016**, *138*, 2174−2177. (b) Qin, T.; Cornella, J.; Li, C.; Malins, L. R.; Edwards, J. T.; Kawamura, S.; Maxwell, B. D.; Eastgate, M. D.; Baran, P. S. *Science* **2016**, *352*, 801−805. (c) Huihui, K. M. M.; Caputo, J. A.; Melchor, Z.; Olivares, A. M.; Spiewak, A. M.; Johnson, K. A.; DiBenedetto, T. A.; Kim, S.; Ackerman, L. K. G.; Weix, D. J. *J. Am. Chem. Soc.* **2016**, *138*, 5016−5019.

(110) (a) Yamashita, Y.; Tellis, J. C.; Molander, G. A. *Proc. Natl. Acad. Sci. U. S. A.* **2015**, *112*, 12026−12029. (b) Ryu, D.; Primer, D.

N.; Tellis, J. C.; Molander, G. A. *Chem. - Eur. J.* **2016**, *22*, 120−123. See also ref 104.

(111) Primer, D. N.; Karakaya, I.; Tellis, J. C.; Molander, G. A. *J. Am. Chem. Soc.* **2015**, *137*, 2195−2198.

(112) (a) Karakaya, I.; Primer, D. N.; Molander, G. A. *Org. Lett.* **2015**, *17*, 3294−3297. (b) Amani, J.; Sodagar, E.; Molander, G. A. *Org. Lett.* **2016**, *18*, 732−735.

(113) El Khatib, M.; Serafim, R. A. M.; Molander, G. A. *Angew. Chem., Int. Ed.* **2016**, *55*, 254−258.

(114) (a) Jouffroy, M.; Primer, D. N.; Molander, G. A. *J. Am. Chem. Soc.* **2016**, *138*, 475−478. (b) Patel, N. R.; Kelly, C. B.; Jouffroy, M.; Molander, G. A. *Org. Lett.* **2016**, *18*, 764−767. (c) Jouffroy, M.; Davies, G. H. M.; Molander, G. A. *Org. Lett.* **2016**, *18*, 1606−1609.

(115) (a) Corcé, V.; Chamoreau, L.-M.; Derat, E.; Goddard, J.-P.; Ollivier, C.; Fensterbank, L. *Angew. Chem., Int. Ed.* **2015**, *54*, 11414−11418. (b) Lévêque, C.; Chenneberg, L.; Corcé, V.; Goddard, J.-P.; Ollivier, C.; Fensterbank, L. *Org. Chem. Front.* **2016**, *3*, 462−465.

(116) Noble, A.; McCarver, S. J.; MacMillan, D. W. C. *J. Am. Chem. Soc.* **2015**, *137*, 624−627. Also see ref 103.

(117) Zuo, Z.; Cong, H.; Li, W.; Choi, J.; Fu, G. C.; MacMillan, D. W. C. *J. Am. Chem. Soc.* **2016**, *138*, 1832−1835.

(118) (a) Chu, L.; Lipshultz, J. M.; MacMillan, D. W. C. *Angew. Chem., Int. Ed.* **2015**, *54*, 7929−7933. Indoles could also be coupled using this strategy; see: (b) Gu, L.; Jin, C.; Liu, J.; Zhang, H.; Yuan, M.; Li, G. *Green Chem.* **2016**, *18*, 1201−1205.

(119) Cheng, W.-M.; Shang, R.; Yu, H.-Z.; Fu, Y. *Chem. - Eur. J.* **2015**, *21*, 13191−13195.

(120) (a) Zhou, C.; Li, P.; Zhu, X.; Wang, L. *Org. Lett.* **2015**, *17*, 6198−6201. (b) Xu, N.; Li, P.; Xie, Z.; Wang, L. *Chem. - Eur. J.* **2016**, *22*, 2236−2242.

(121) Le, C. C.; MacMillan, D. W. C. *J. Am. Chem. Soc.* **2015**, *137*, 11938−11941.

(122) Joe, C. L.; Doyle, A. G. *Angew. Chem., Int. Ed.* **2016**, *55*, 4040−4043.

(123) (a) Lang, S. B.; O'Nele, K. M.; Tunge, J. A. *J. Am. Chem. Soc.* **2014**, *136*, 13606−13609. (b) Lang, S. B.; O'Nele, K. M.; Douglas, J. T.; Tunge, J. A. *Chem. - Eur. J.* **2015**, *21*, 18589−18593.

(124) Xuan, J.; Zeng, T.-T.; Feng, Z.-J.; Deng, Q.-H.; Chen, J.-R.; Lu, L.-Q.; Xiao, W.-J.; Alper, H. *Angew. Chem., Int. Ed.* **2015**, *54*, 1625−1628.

(125) Shaw, M. H.; Shurtleff, V. W.; Terrett, J. A.; Cuthbertson, J. D.; MacMillan, D. W. C. *Science* **2016**, *352*, 1304−1308.

(126) Zhang, P.; Le, C. C.; MacMillan, D. W. C. *J. Am. Chem. Soc.* **2016**, *138*, 8084.

(127) Macgregor, S. A.; Neave, G. W.; Smith, C. *Faraday Discuss.* **2003**, *124*, 111−127.

(128) (a) Matsunaga, P. T.; Hillhouse, G. L.; Rheingold, A. L. *J. Am. Chem. Soc.* **1993**, *115*, 2075−2077. (b) Matsunaga, P. T.; Mavropoulos, J. C.; Hillhouse, G. L. *Polyhedron* **1995**, *14*, 175−185. (c) Han, R.; Hillhouse, G. L. *J. Am. Chem. Soc.* **1997**, *119*, 8135−8136.

(129) Terrett, J. A.; Cuthbertson, J. D.; Shurtleff, V. W.; MacMillan, D. W. C. *Nature* **2015**, *524*, 330−334.

(130) Tasker, S. Z.; Jamison, T. F. *J. Am. Chem. Soc.* **2015**, *137*, 9531−9534.

(131) Corcoran, E. B.; Pirnot, M. T.; Lin, S.; Dreher, S. D.; DiRocco, D. A.; Davies, I. W.; Buchwald, S. L.; MacMillan, D. W. C. *Science* **2016**, DOI: 10.1126/science.aag0209.

(132) (a) Surry, D. S.; Buchwald, S. L. *Chem. Sci.* **2011**, *2*, 27−50. (b) Fors, B. P.; Watson, D. A.; Biscoe, M. R.; Buchwald, S. L. *J. Am. Chem. Soc.* **2008**, *130*, 13552−13554. (c) Hartwig, J. F. *Synlett* **1997**, *1997*, 329−340. (d) Brusoe, A. T.; Hartwig, J. F. *J. Am. Chem. Soc.* **2015**, *137*, 8460−8468.

(133) Yoo, W.-J.; Tsukamoto, T.; Kobayashi, S. *Angew. Chem., Int. Ed.* **2015**, *54*, 6587−6590.

(134) Choi, S.; Chatterjee, T.; Choi, W. J.; You, Y.; Cho, E. J. *ACS Catal.* **2015**, *5*, 4796−4802.

(135) Jouffroy, M.; Kelly, C. B.; Molander, G. A. *Org. Lett.* **2016**, *18*, 876−879.

(136) Oderinde, M. S.; Frenette, M.; Robbins, D. W.; Aquila, B.; Johannes, J. W. *J. Am. Chem. Soc.* **2016**, *138*, 1760−1763.

(137) Xuan, J.; Zeng, T.-T.; Chen, J.-R.; Lu, L.-Q.; Xiao, W.-J. *Chem. - Eur. J.* **2015**, *21*, 4962−4965.

(138) Zhang, G.; Liu, C.; Yi, H.; Meng, Q.; Bian, C.; Chen, H.; Jian, J.-X.; Wu, L.-Z.; Lei, A. *J. Am. Chem. Soc.* **2015**, *137*, 9273−9280.

(139) (a) Gao, X.-W.; Meng, Q.-Y.; Li, J.-X.; Zhong, J.-J.; Lei, T.; Li, X.-B.; Tung, C.-H.; Wu, L.-Z. *ACS Catal.* **2015**, *5*, 2391−2396. (b) Zhong, J.-J.; Wu, C.-J.; Meng, Q.-Y.; Gao, X.-W.; Lei, T.; Tung, C.-H.; Wu, L.-Z. *Adv. Synth. Catal.* **2014**, *356*, 2846−2852. (c) Xiang, M.; Meng, Q.-Y.; Li, J.-X.; Zheng, Y.-W.; Ye, C.; Li, Z.-J.; Chen, B.; Tung, C.-H.; Wu, L.-Z. *Chem. - Eur. J.* **2015**, *21*, 18080−18084.

(140) (a) Loupy, A.; Tchoubar, B.; Astruc, D. *Chem. Rev.* **1992**, *92*, 1141−1165. (b) Goodson, B.; Schuster, G. B. *Tetrahedron Lett.* **1986**, *27*, 3123−3126.

(141) Fukuzumi, S.; Kojima, T. *JBIC, J. Biol. Inorg. Chem.* **2008**, *13*, 321−333.

(142) (a) Du, J.; Yoon, T. P. *J. Am. Chem. Soc.* **2009**, *131*, 14604−14605. (b) Tyson, E. L.; Farney, E. P.; Yoon, T. P. *Org. Lett.* **2012**, *14*, 1110−1113.

(143) Lu, Z.; Shen, M.; Yoon, T. P. *J. Am. Chem. Soc.* **2011**, *133*, 1162−1164.

(144) Zhao, G.; Yang, C.; Guo, L.; Sun, H.; Lin, R.; Xia, W. *J. Org. Chem.* **2012**, *77*, 6302−6306.

(145) Hurtley, A. E.; Cismesia, M. A.; Ischay, M. A.; Yoon, T. P. *Tetrahedron* **2011**, *67*, 4442−4448.

(146) Du, J.; Skubi, K. L.; Schultz, D. M.; Yoon, T. P. *Science* **2014**, *344*, 392−396.

(147) Amador, A. G.; Sherbrook, E. M.; Yoon, T. P. *J. Am. Chem. Soc.* **2016**, *138*, 4722−4725.

(148) For an example of α-amine functionalization which utilizes dual photoredox Lewis acid catalysis, see: Zhu, S.; Rueping, M. *Chem. Commun.* **2012**, *48*, 11960−11962.

(149) Yang, Z.; Li, H.; Zhang, L.; Zhang, M.-T.; Cheng, J.-P.; Luo, S. *Chem. - Eur. J.* **2015**, *21*, 14723−14727.

(150) Huo, H.; Harms, K.; Meggers, E. *J. Am. Chem. Soc.* **2016**, *138*, 6936−6939.

(151) Huo, H.; Shen, X.; Wang, C.; Zhang, L.; Röse, P.; Chen, L.-A.; Harms, K.; Marsch, M.; Hilt, G.; Meggers, E. *Nature* **2014**, *515*, 100−103.

(152) Huo, H.; Wang, C.; Harms, K.; Meggers, E. *J. Am. Chem. Soc.* **2015**, *137*, 9551−9554.

(153) Wang, C.; Zheng, Y.; Huo, H.; Röse, P.; Zhang, L.; Harms, K.; Hilt, G.; Meggers, E. *Chem. - Eur. J.* **2015**, *21*, 7355−7359.

(154) Tan, Y.; Yuan, W.; Gong, L.; Meggers, E. *Angew. Chem., Int. Ed.* **2015**, *54*, 13045−13048.

(155) Wang, C.; Qin, J.; Shen, X.; Riedel, R.; Harms, K.; Meggers, E. *Angew. Chem., Int. Ed.* **2016**, *55*, 685−688.

(156) Douglas, J. J.; Sevrin, M. J.; Stephenson, C. R. J. *Org. Process Res. Dev.* **2016**, DOI: 10.1021/acs.oprd.6b00125.

(157) Lin, S.; Ischay, M. A.; Fry, C. G.; Yoon, T. P. *J. Am. Chem. Soc.* **2011**, *133*, 19350−19353.

(158) Lin, S.; Padilla, C. E.; Ischay, M. A.; Yoon, T. P. *Tetrahedron Lett.* **2012**, *53*, 3073−3076.

(159) Furst, L.; Narayanam, J. M. R.; Stephenson, C. R. J. *Angew. Chem., Int. Ed.* **2011**, *50*, 9655−9659.

(160) Schnermann, M. J.; Overman, L. E. *J. Am. Chem. Soc.* **2011**, *133*, 16425−16427.

(161) Schnermann, M. J.; Untiedt, N. L.; Jiménez-Osés, G.; Houk, K. N.; Overman, L. E. *Angew. Chem., Int. Ed.* **2012**, *51*, 9581−9586.

(162) Miyazawa, K.; Koike, T.; Akita, M. *Adv. Synth. Catal.* **2014**, *356*, 2749−2755.

(163) Douglas, J. J.; Cole, K. P.; Stephenson, C. R. J. *J. Org. Chem.* **2014**, *79*, 11631−11643.

(164) Kutchukian, P. S.; Dropinski, J. F.; Dykstra, K. D.; Li, B.; DiRocco, D. A.; Streckfuss, E. C.; Campeau, L.-C.; Cernak, T.; Vachal, P.; Davies, I. W.; Krska, S. W.; Dreher, S. D. *Chem. Sci.* **2016**, *7*, 2604−2613.

(165) Nagib, D. A.; MacMillan, D. W. C. *Nature* **2011**, *480*, 224−228.

(166) DiRocco, D. A.; Dykstra, K.; Krska, S.; Vachal, P.; Conway, D. V.; Tudge, M. *Angew. Chem., Int. Ed.* **2014**, *53*, 4802−4806.

(167) Cambié, D.; Bottecchia, C.; Straathof, N. J. W.; Hessel, V.; Noël, T. *Chem. Rev.* **2016**, DOI: 10.1021/acs.chemrev.5b00707.

(168) Borman, S. *Chem. Eng. News* **2015**, *93* (29), 33−34.

(169) Beatty, J. W.; Douglas, J. J.; Cole, K. P.; Stephenson, C. R. J. *Nat. Commun.* **2015**, *6*, 7919.

(170) Yayla, H. G.; Peng, F.; Mangion, I. K.; McLaughlin, M.; Campeau, L.-C.; Davies, I. W.; DiRocco, D. A.; Knowles, R. R. *Chem. Sci.* **2016**, *7*, 2066−2073.

(171) Yoo, W.-J.; Tsukamoto, T.; Kobayashi, S. *Org. Lett.* **2015**, *17*, 3640−3642.